HHS Public Access

Author manuscript

Nat Microbiol. Author manuscript; available in PMC 2022 May 22.

Published in final edited form as:

Nat Microbiol. 2021 December ; 6(12): 1493–1504. doi:10.1038/s41564-021-00983-z.

Mycobiota-induced IgA antibodies regulate fungal commensalism in the gut and are dysregulated in Crohn's Disease

Itai Doron[1,2], **Marissa Mesko**[1,2], **Xin V. Li**[1,2], **Takato Kusakabe**[1,2], **Irina Leonardi**[1,2], **Dustin G. Shaw**[4], **William D. Fiers**[1,2], **Woan-Yu Lin**[1,2,6], **Meghan Bialt-DeCelie**[1,2], **Elvira Román**[3], **Randy S. Longman**[1,2,6], **Jesus Pla**[3], **Patrick C. Wilson**[4], **Iliyan D. Iliev**[1,2,5,6,*]

[1]Gastroenterology and Hepatology Division, Joan and Sanford I. Weill Department of Medicine, Weill Cornell Medicine, New York, NY 10021, USA.

[2]The Jill Roberts Institute for Research in Inflammatory Bowel Disease, Weill Cornell Medicine, New York, NY 10021, USA.

[3]Department of Microbiology and Parasitology-IRYCIS, Faculty of Pharmacy, Universidad Complutense de Madrid, 28040 Madrid, Spain

[4]Department of Medicine, Section of Rheumatology, the Knapp Center for Lupus and Immunology, University of Chicago, Chicago IL.

[5]Department of Microbiology and Immunology, Weill Cornell Medicine, New York, NY 10065, USA.

[6]Immunology and Microbial Pathogenesis Program, Weill Cornell Graduate School of Medical Sciences, Weill Cornell Medicine, Cornell University, New York, NY 10065, USA

Abstract

Secretory immunoglobulin A (sIgA) plays an important role in gut barrier protection by shaping the resident microbiota community, restricting the growth of bacterial pathogens, and enhancing host protective immunity via immunological exclusion. Here, we found that a portion of microbiota-driven sIgA response is induced by and directed towards intestinal fungi. Analysis of the human gut mycobiota bound by sIgA revealed a preference for hyphae; a fungal morphotype associated with virulence. *C. albicans* was a potent inducer of IgA class switch recombination (CSR) among plasma cells, through an interaction dependent on intestinal phagocytes and hyphal programming. Characterization of sIgA affinity and polyreactivity showed that hyphae-associated virulence factors were bound by these antibodies and that sIgA influenced *C. albicans*

*Correspondence to: iliev@med.cornell.edu.

Author contribution

I.D. and I.D.I. conceived and designed experiments, I.D., M.M., D.G.S., X. V. L., I.L., T.K, W.D.F., W.Y.L., E.R. and M.B.C. performed experiments. J.P., R.S.L. and P.C.W., generated key research materials and contributed to experiment interpretation. I.D. and I.D.I. generated figures and legends from analyzed data. I.D.I acquired funding for the project. I.D. and I.D.I. wrote the manuscript.

Competing Interests

The authors declare no competing interests related to this study.

morphotypes in the murine gut. Furthermore, an increase of granular hyphal morphologies in Crohn's Disease (CD) patients compared to healthy controls, correlated with a decrease of antifungal sIgA antibody titers with affinity to hyphae-associated virulence factors. Thus, in addition to their importance in gut bacterial regulation, sIgA targets the uniquely fungal phenomenon of hyphal formation. Our findings indicate that antifungal sIgA produced in the gut can play a role in regulating intestinal fungal commensalism by coating fungal morphotypes linked to virulence, thereby providing a protective mechanism that might be dysregulated in CD patients.

Keywords

Mycobiome; IgA Antibodies; Crohn's Disease; Fungal commensalism; Hyphae; *Candida albicans*

Introduction

Immunoglobulin A (IgA) is the most prominent antibody in the human intestinal lumen – 3–5 grams are secreted daily – and coats the majority of the intestinal bacterial community[1–5]. In health and disease, the binding of secretory IgA (sIgA) modulates intestinal immunity and homeostasis through a variety of mechanisms, including crosslinking microbiota in the lumen to prevent encroachment on the intestinal epithelium, shuttling bound microbes to secondary lymphoid tissues, binding toxins, and directly modulating microbial metabolic activity[1–3,6–12]. Intestinal sIgA primarily originates from long-lived plasma B cells in response to commensal, host, and dietary antigens: a process that takes place in several intestinal tissues through the involvement of T cell-independent (TI) and T cell-dependent (TD) pathways[3,6–11]. In addition to common "public" B cell clonotypes detectable also in germ-free mice, B cell clonotypes producing sIgA with specificity to bacteria that are dependent on the gut microbiota are commonly found in the gut[6,13,14]. Single B cell repertoire and monoclonal antibody reactivity analyses have revealed that the IgA^+ gut plasma cells induced by microbiota gut colonization undergo significant affinity maturation to generate commensal bacteria-specific sIgA antibodies[1,13,15]. The identification of highly immunogenic commensal bacteria through a combination of sIgA binding-based microbial flow cytometry, 16S amplicon sequencing, and the presence of sIgA targeted bacterial epitopes have further elucidated our understanding of the mechanisms governing gastrointestinal balance and how dysbiosis can drive intestinal pathologies[16,17]. Despite these exciting developments in bacterial-sIgA biology, the potential involvement of the fungal component of the gut microbiota (mycobiota) in these processes is largely unknown. Only recently have intestinal fungi been recognized as a factor contributing to inflammatory disease or response to therapy[18–25] prompting multiple questions regarding antifungal mucosal antibody response specificity, function, and mechanisms of induction in the gut.

Antibodies against yeast mannan (ASCA) with unknown function develop in Crohn's Disease patients (CD)[26–28], where fungal dysbiosis and overgrowth of *Candida* species have been consistently described[18–21]. We have shown that polymorphisms in the fractalkine receptor gene *CX3CR1* are associated with a substantial decrease of antifungal antibodies in CD patients, while the depletion of $CX3CR1^+$ macrophages in mice exacerbated intestinal

disease following fungal colonization[24]. These findings suggest a possible link between antibody-mediated immunity, mycobiota, and intestinal disease.

In contrast to most bacteria, many fungal species are capable of dramatically changing cellular morphologies into functionally and compositionally distinct morphotypes in response to environmental and host changes. Recent studies also demonstrate that sIgA in the heathy human gut and oral mucosa bind to specific fungal species[29,30]. During homeostasis commensal fungi similar to commensal bacteria interact with the host in mutualistic ways[29,31–33], raising a question of how fungal commensalism in the gastrointestinal tract is maintained. We hypothesized that exposure to morphotype-dependent fungal factors and their interactions with sIgA in the gut regulates fungal commensal states.

Results

A subset of gut mycobiota is coated by secretory IgA induced predominantly by *C. albicans*.

To visualize fungal cells in the intestines, murine feces from C57BL/6J mice housed in our facility[34] were stained with DNA-binding SYBR-Green (SYBR) to distinguish live microbes from $Sybr^{lo}$ debris and microbial components found in sterilized food and cage bedding (Extended Data Fig. 1a). Co-staining with the chitin-binding calcofluor-white (CFW) dyes distinguished the $CFW^{+}Sybr^{hi}$ fungal population within the $Sybr^{hi}$ microbial populations as a whole (Extended Data Fig. 1b)[29]. The material was then stained with fluorescently labeled anti-IgA, anti-IgM and anti-IgG antibodies to visualize the intestinal fungi-bound antibody repertoire. Consistent with luminal sIgA abundance and previous assessments of intestinal bacteria-bound antibody repertoires[1–3,6–11,35], this approach revealed a large fraction of intestinal fungi bound by sIgA (Fig. 1a, b). Neither sIgG nor sIgM fungal binding was observed in the gut (Fig. 1a, b), reflecting a lack of IgG and IgM transcytosis in the adult mammalian intestine[1–5] and distinguishing IgA as the primary immunoglobulin contributing to intestinal homeostasis during steady-state. The presence of antifungal sIgA was dependent upon the presence of mature functional B cells, as these antibodies were absent in the lumen of both B cell-deficient $\mu MT^{-/-}$ and B/T cell-deficient cell $Rag1^{-/-}$ mice (Fig. 1c, d). Notably, the lack of an antifungal sIgA response in $\mu MT^{-/-}$ mice negates the contribution of unconventional IgA induction pathways through peritoneal B cells[11,36]. Similar results were obtained upon assessment of the fecal mycobiota of healthy human subjects (Fig. 1 e, f), suggesting that significant antifungal sIgA binding of gut mycobiota occurs in both mice and humans.

While sIgA can be induced by both food antigens and the gut microbiota, and total IgA levels continuously increase with age in both germ-free (GF) and colonized mice[37,38], monocolonization experiments have consistently demonstrated that a fraction of sIgA is both microbiota-induced and microbiota-reactive[1,3,4,6,7,37,39]. Having previously demonstrated that the gut mycobiota contributes to the host circulating IgG antibody pool[29], we next investigated whether intestinal fungi contribute to the antifungal sIgA repertoire observed under steady-state. Fungal monocolonization experiments were performed in GF mice using several fungal species found in the human or the murine gut[29]. Surprisingly, among those, *C.*

albicans was the species that induced a robust luminal sIgA response (Fig. 1g). sIgA binding to *C. albicans* cells was already detectible during early colonization and increased over time (Fig. 1h) consistent with the course of sIgA production induced by this fungus (Extended Data Fig. 1c). These results were corroborated upon analysis of the Peyer's patches (PP) of *C. albicans*-colonized mice where we observed a significant increase in IgA^+ frequency in the B cell compartment relative to non-colonized GF mice (Fig. 1i, Extended Data Fig. 1d).

Bacterial composition can dramatically influence fungal colonization in the gut[23,40,41]. To assess the potential role of intestinal bacteria in this process, we next utilized altered Schaedler flora (ASF)-colonized mice that carry a defined set of bacteria but are mycobiota-free[42,43]. Consistent with our findings in GF mice, intestinal colonization with *C. albicans* correlated with increased frequencies of IgA^+ B cells in the PP (Fig. 1j, k). Notably, within the germinal center B cell (GC-B) subset, which consists of highly proliferative mature B cells that are undergoing affinity maturation and associated with high-affinity antibody responses, the same patterns of increased IgA CSR were observed (Fig.1l, m). Together, these results suggest that *C. albicans* intestinal colonization induces strong IgA class-switch recombination (CSR) responses in the PPs independent of the presence of intestinal bacteria.

Antifungal sIgA antibodies direct fungal commensalism by preferentially targeting hyphal morphotypes

In contrast to bacteria, fungal cells express specific morphotypes in the gut[31] – yeast and hyphae – that differ in both cell size and function. An analysis of fungal cells size and granularity in $sIgA^+$ and $sIgA^-$ fractions (based on forward and side scatter) revealed enrichment of larger and more granular fungi in the sorted sIgA-bound fraction relative to unbound fungal cells or fungi in unsorted material overall (Fig. 2a–c, Extended Data Fig. 2a–e), suggesting a preferential binding of sIgA to specific fungal morphologies. *C. albicans* is the most abundant and common dimorphic fungus in the human GI tract, is present in IBD patients[18] and was recently demonstrated to be capable of producing pseudohyphae upon intestinal colonization[31]. Because *C. albicans* made up the majority of fungi found in both $sIgA^+$ and $sIgA^-$ fractions in the assessed human fecal samples[29], but larger and more granular fungal cells were preferably bound to sIgA (Fig. 2a–c), we hypothesized that sIgA preferentially binds fungal hyphae. Thus, we used human fecal slurry as a source of sIgA to stain *C. albicans*. To observe morphological differences in *C. albicans* antifungal sIgA binding *in vitro* or *in vivo*, we generated double reporter *C. albicans* strain (Ca-dREP) in which the enolase 1 (*ENO1*) promoter was used to constitutively express relatively high amounts of GFP resulting in green fungal cells (Extended Data Fig. 3, GFP), while RFP was expressed under hyphal wall protein 1 gene (*HWP1*) promoter resulting in strong RFP expression specifically in hyphae during filamentation (Extended Data Fig. 3, RFP). Using human fecal slurry as a source of sIgA, we first investigated sIgA binding upon incubation with *in vitro* cultures of this double reporter mutant. Analysis by fluorescent microscopy revealed preferential sIgA hyphae coating, while yeast cells were targeted significantly less (Fig. 2d–f; Extended Data Fig. 3a, b top rows). The same staining approach utilizing feces from *C. albicans*-colonized IgA-sufficient or IgA-deficient $Rag1^{-/-}$ mice revealed similar preferential coating of *C. albicans* hyphae by murine sIgA (Fig. 2g, h). As expected, this phenomenon was dependent on the presence of functional lymphocytes (Fig. 2g, h).

Deficiency in the *Candida albicans* morphogenesis program in the gut is considered a key determinant of commensalism[31–33,44]. Consistent with previous reports[31,45–47], co-colonization of specific pathogen free (SPF) WT mice that are naturally naïve to *C. albicans*[40] with a 1:1 mixture of hyphae-sufficient and hyphal formation-impaired *efg1Δ/Δ C. albicans* mutant resulted in decreased fitness of the hyphae-sufficient strain (Fig. 2i). Notably, we observed the opposite result in *Rag1*$^{-/-}$ mice (Fig. 2j), suggesting that adaptive immunity-dependent features might play a role in regulating *C. albicans* commensalism in the gut.

In light of these results and the observed morphological dependency of sIgA binding *in vitro*, we sought to investigate whether this phenomenon occurs *in vivo* and whether sIgA plays any role in *C. albicans* morphogenesis and commensal states in the gut. sIgA-sufficient (WT) and deficient (*Rag1*$^{-/-}$ and *μMT*$^{-/-}$) mice were colonized with Ca-dREP for four and fourteen days, after which colon contents were assessed by flow cytometry for frequency of RFP^{+} hyphae. Notably, in both *Rag1*$^{-/-}$ and *μMT*$^{-/-}$ mice, a higher frequency of hyphae was detected within the colonized Ca-dREP population relative to similarly colonized WT control mice (Fig. 2k, l). Furthermore, sIgA binding assessment of the WT mice colonized with Ca-dREP recapitulated the sIgA binding results observed *in vitro* (Fig. 2g, h), with significantly higher frequencies of sIgA binding observed among hyphal Ca-dREP relative to yeast morphology at both early and later stages of colonization with an increase at the later time point (Fig. 2m–o), consistent with the course of free sIgA production (Extended Data Fig. 1c) and binding (Fig. 1h) to *C. albicans*. To assess whether a similar phenomenon takes place in humans, we isolated sIgA from healthy human feces that was applied to the two-partner system of Ca-dREP and intestinal epithelial cell line Caco-2 (used as an inducer of hyphal morphogenesis[48]). Consistently, sIgA treatment limited the frequency of *C. albicans* hyphal morphologies in this assay while complimentary increase of yeast morphotype frequencies was observed (Fig. 2p, q). Together, these data suggest that the absence of gut antifungal sIgA antibodies result in increased hyphal morphogenesis of *C. albicans*, implicating a role for sIgA in maintaining *C. albicans* commensalism.

Hyphal morphotypes drive the robust *C. albicans*-induced sIgA responses

We next engineered hyphae-competent (WT) and hyphae-deficient (yeast-locked; *efg1Δ/Δ cph1Δ/Δ* strain[49,50]) strains of *C. albicans* to express RFP or GFP, respectively, both to further explore preferential sIgA binding to hyphae *in vivo* and to assess differences in sIgA repertoires induced in the presence or absence of the hyphal morphology. WT mice were colonized with a 1:1 mixture of hyphae-competent (WT) and hyphae-deficient (yeast-locked; *efg1Δ/Δ cph1Δ/Δ* strain[49,50]) strains of *C. albicans* that could be later detected in fecal material (Fig. 3a). Consistently, hyphae-competent WT *C. albicans* strain was bound by sIgA with higher frequency when compared to the co-colonized yeast-locked strain (Fig. 3b, c).

To explore the mechanisms behind sIgA induction, we next colonized mice with hyphae sufficient WT or yeast-locked *efg1Δ/Δ cph1Δ/Δ C. albicans* strains (Extended Data Fig. 3c). Interestingly, hyphae-sufficient *C. albicans* induced significantly more IgA^{+} CSR in the B cells of the PPs than the *efg1Δ/Δ cph1Δ/Δ* strain, despite greater expansion of the

later in the murine gut (Fig. 3d–f). Since polyreactivity is a common trait identified in recent characterizations of gut sIgA repertoires[7], hyphae-induced IgA CSR could either be inducing antibodies that bind cellular structures common to fungi and present in all *C. albicans* morphotypes or exhibit specific reactivity to hyphae-associated virulence factors. We therefore colonized "mycobiota-naïve" ASF mice with *C. albicans* and assessed sIgA reactivity against cell lysates derived from either yeast-locked or hyphae-sufficient *C. albicans*. This assessment revealed a preference of sIgA to lysates of hyphal *C. albicans* as compared to those of the hyphal deficient strain (Fig. 3g). Notably, no morphotype-specific preference was observed in *efg1Δ/Δ cph1Δ/Δ* colonized mice or fungi-naïve ASF controls (Fig. 3g). Altogether this data suggests that hyphal morphotypes of *C. albicans* are potent inducers of antifungal sIgA and that such antibodies sway fungal commensalism by preferentially targeting hyphal morphotypes.

sIgA responses to *C. albicans* hyphal morphotypes are mediated through innate immune interaction with intestinal phagocytes

Several intestinal populations of phagocytes play important roles in microbiota regulation, barrier protection, priming of antigen specific responses to microbial antigens and regulation of sIgA responses to intestinal microbes[17,51,52]. Recent findings suggest that a population of mononuclear phagocytes that express high levels of the fractalkine receptor CX3CR1 (CX3CR1$^+$ MNPs)[53,54] are both involved in IgA responses to bacteria[52] and are central to fungal sensing and priming of antifungal T cell responses in the intestines[24,42], and play a role in the protection of intestinal epithelial cells from fungal toxins[55]. A loss-of-function mutation in *CX3CR1*, leads to loss of systemic antifungal IgG responses in humans and mice[24,29]. On the other hand, CD11c$^+$CD11b$^+$CD103$^+$ dendritic cells (DCs) that developmentally depend on the transcription factor IRF4[52,56,57], have been long known to play an important role in the PPs and control of IgA responses to bacterial and food antigens in the small intestine[58,59].

The PP in the small intestine play a key role in the induction of sIgA responses specific to penetrant commensals and invasive pathogens[6,60], while lamina propria and adjacent isolated lymphoid follicle-produced sIgA targets both invasive and non-invasive bacteria as well as food antigens[4,6,7,60,61]. A recent study demonstrated that a subset of CX3CR1$^+$ MNPs that are required for the development of tertiary lymphoid structures (TLSs) in the colon serve as a site for Salmonella-specific IgA response[52]. Because intestinal colonization with *C. albicans* that lead to sIgA production (Fig. 3h), induced an increase of IgA$^+$ B cells in the PPs and in the lamina propria (Fig. 3i–k, Extended Data Fig. 4a, b), we next explored if either of these two populations of gut-resident phagocytes play any role in the induction of antifungal sIgA in PPs and in the lamina propria. We generated ΔCX3CR1 mice (Cx3cr1^{DTR} × CD11c^{Cre}) to selectively deplete intestinal CX3CR1$^+$ MNPs. To selectively target CD11c$^+$CD11b$^+$CD103$^+$ DCs (cDC2), we crossed flox-inducible Irf4$^{fl/fl}$ allele mice with transgenic Cd11c^{Cre} mice (ΔIrf4). Intestinal colonization of ΔIrf4 mice and respective littermates with hyphae-sufficient *C. albicans* revealed a reliance of anti-*C. albicans* sIgA production and *C. albicans*-dependent induction of IgA$^+$ B cells in the PPs on cDC2 as previously described for bacteria[55,56] (Fig. 4a–d). Targeting of CX3CR1$^+$ MNPs on the other hand affected *C. albicans*-dependent induction of IgA$^+$ B cells in the lamina propria

without affecting these cells in the PPs (Fig. 4e–h). Notably, depletion of either phagocyte population lead to a decrease of luminal anti-*Candida* sIgA (Fig. 4d, h) that coincided with an increase of granular fungal morphologies in the gut (Fig. 4i–l; Extended Data Fig. 4c; Extended Data Fig. 2). Altogether the data suggest that cDC2 and CX3CR1^{+} MNPs might be interdependent by regulating different pathways of antifungal sIgA induction: one affecting the IgA^{+} B cells in the PPs while the other affecting IgA^{+} plasmablasts in the LP.

C. albicans-induced sIgA targets hyphae-associated virulence factors.

As one of the most successful fungal opportunists *C. albicans* has evolved to survive in the gut or invade host tissues: a process associated with yeast-to-hyphal transition[50,62,63]. Among several key virulence factors, hyphae-produced proteins such as secreted aspartyl proteinases (specifically Sap6 in the gut[31]), agglutinin-like protein 3 precursor (Als3)[64] and *Ece1*-derived cytolytic toxin candidalysin (Ece1-III)[65] have been implicated in tissue adhesion and damage associated with fungal pathogenesis. Thus, we next explored whether hyphae-reactive sIgA induced by *C. albicans* intestinal colonization (Fig. 5a) was driven by reactivity to these virulence factors. While sIgA exhibited only a minimal binding to cell wall mannan (Fig. 5b), these antibodies were distinguished by significant increase in reactivity to candidalysin and by significant but lesser extent to Sap6 (Fig. 5c–d). Furthermore, anti-bacterial flagellin sIgA titers in mice were not affected by *C. albicans* colonization (Fig. 5e), suggesting fungal reactivity of *C. albicans* induced sIgA antibodies.

Increase of granular hyphal morphologies and dysregulated antifungal sIgA responses are observed in Crohn's Disease.

Given these findings and since we found that the hyphal program is involved in the induction of antifungal sIgA, we next explored whether intestinal inflammation affects antifungal sIgA in the human intestinal mucosa where these antibodies are produced. Thus, we focused these investigations on CD as a disease where serum circulating antibodies against fungal mannan (anti-*S. cerevisiae* antibodies; ASCA) are elevated and used as marker of disease severity[26–28]. We examined mucosal intestinal washings and serum from healthy controls and CD patients. As expected, circulating ASCA IgA and IgG antibodies were increased in CD compared to controls, while differential increase of these antibodies did not reach statistical significance in mucosal washings of CD patients in our cohort (Fig. 5f, g). In contrast, sIgA antibodies reactive to *Candida* hyphae-produced proteins such as Sap6 and candidalysin were decreased (Fig. 5h–i). Consistent with dysregulation of antibody responses, flow cytometry-based analysis revealed an increase of granular fungal morphologies in CD mucosal washings (Fig. 5j). These data suggest that dysregulated antibody response against factors produced by hyphal morphotypes and an increase of hyphal morphologies in the mucosa might be occurring during CD.

Altogether the data indicate that while human sIgA with reactivity to both yeast and hyphal morphotypes exist in the human gut, sIgA with preferential binding to hyphae might arise in response to specific hyphae-associated virulence factors (Extended Data Fig. 5). Furthermore, Crohn's disease might alter this process by affecting the targeting of hyphae-associated virulence factors by sIgA that can influence specific fungal morphotypes associated with fungal virulence.

Discussion

In addition to the intestinal mucus layer and antimicrobial peptides, sIgA antibodies have long been considered an important player in intestinal homeostasis by providing a "first line" of defense against invasive pathogens, toxins or other harmful food and metabolic bacterial products. Here, we describe that a fraction of sIgA present in the intestinal lumen is directed towards fungi. It has been previously established that sIgA displays broad cross-bacterial reactivity with occasional preferential coating of distinct bacterial species[4,7,8,16,17,66–68]. Here, we discovered that a phenomenon specific to the fungal kingdom, namely the ability to produce hyphae, was the main target of sIgA antifungal antibodies. We found that among several gut fungal species *C. albicans* and its hyphal morphotype was a key target and the most potent inducer of antifungal sIgA, suggesting that selected fungal species and specific morphotypes are involved in its induction (Extended Data Fig. 5). Since multiple fungal species are capable of hyphae or pseudohyphae formation[30,31,49,69–77], future research should determine whether this is due to an inability of specific fungi to produce hyphae in the intestinal environment, a requirement of specific virulence factors and metabolites, or a combination of all of the above.

As hyphal formation is a primary mechanism used by dimorphic fungi to invade and translocate between environments within their hosts[69], targeting of these structures might have important functional consequences to fungal commensalism, fungal pathogenesis and immune responses to these processes by the host. Indeed, here we show that the absence of sIgA potentiates hyphal growth in the murine intestines. Altogether our findings, and recent findings by others[78], suggest that the ability to thrive in the gut[31,32,46] a switch between specific fungal morphotypes (and switch between commensal vs pathobiont states) and associated production of virulence factors might all be involved in the capacity of *C. albicans* to induce sIgA, and that antifungal sIgA play a role in control of fungal commensalism in the gut.

While ITS sequencing methodologies are successfully used to explore the mycobiota composition in different IBD cohorts, changes in specific fungal genera are inconsistently observed across cohorts[18–24]. Our findings suggest that an assessment of additional parameters (Fig. 5g–j) might provide a better understanding of the role of the gut mycobiota in IBD.

Despite an inability to efficiently track yeast-to-hyphae transition and IgA binding (facilitated by the use of Ca-dREP in mice) in humans as well as the limitation of using an individual cohort, we found that sIgA antibodies that bind to hyphae-associated factors are decreased in CD patients (Extended Data Fig. 5) where *Candida* species expansion has been reported[18–21]. While studies in multiple cohorts demonstrate that systemic antibodies against yeast mannan (ASCA) consistently develop in CD patients[22,26–28], our findings suggest a potentially differential role for systemic and secretory antibodies in this patient population that warrants further investigation, which may lead to a better understanding of mycobiota involvement in the pathogenesis of human inflammatory diseases.

Experimental Model and Subject Details

Ethics

All mouse experiments were performed after prior approval by the Institutional Animal Care and Use Committee of Weill Cornell Medicine. Human fecal samples or mucosal washings from healthy and Crohn's Disease affected de-identified individuals were obtained with informed consent following Institutional-Review-Board-approved protocols at Weill Cornell Medicine.

Contact for reagents, data, resource sharing and code availability statement

All data needed to evaluate the conclusions in the manuscript are available within the main text or supplementary materials. Further information and requests for resources and reagents should be directed to and will be fulfilled by the Lead Contact. No custom code was used.

Mice

7–8-week-old wildtype (WT) C57BL/6J, *Ighm*^{tm1Cgn}/J (*μMT*$^{-/-}$), *Rag1*^{tm1Mom} (*Rag1*$^{-/-}$), Tg(Itgax-cre)1–1Reiz (*Cd11c-cre), Irf4*^{tm1Rdf}(*Irf4*$^{fl/fl}$), and *Cx3cr*$^{1tm\ (DTR)Litt/J}$ (*Cx3cr1*^{DTR}) mice were purchased from the Jackson Laboratories (Bar Harbor, ME, supplementary Table S1). *Irf4*$^{fl/fl}$ or *Cx3cr1*^{DTR} were bred with hemizygous Cd11c-cre$^{+/-}$ for selective depletion of CD11c^{+} CD11b^{+} CD103^{+} DCs (ΔIRF4 mice) or CD11c^{+} CD11b^{+} CX3CR1^{+} MNPs after administration of diphtheria toxin (DT) in the latter case. Depletion was achieved in *Cd11c-cre*$^{+/-}$ *Cx3cr1*^{DTR}, but not *Cd11c-cre*$^{-/-}$ *Cx3cr1*^{DTR} littermates, by injection or three consecutive days with 100ng of DT i.p. followed by maintenance injection every other day for the length of the experiments. Depleted mice were designated as ΔCX3CR1 mice. Mice breed for several generations and maintained under SPF condition at a designated room at the WCM animal facility are referred to as SPF WT WCM-CE mice, while mice purchased from the Jackson Laboratories (Bar Harbor, ME) and used for experiments right after are referred to as SPF WT JAX mice. All experimental animals were used at 8–16 weeks old, and experimental groups included mice split into equal ratios of male and female. No statistical methods were used to pre-determine sample sizes, but our sample sizes are similar to those reported in previous publications[8,29,78]. Mice were housed under specific pathogen-free (SPF) conditions unless otherwise described at Weill Cornell Medicine.

Germ-free (GF) C57BL/6 mouse colonies were maintained within sterile vinyl isolators at Weill Cornell Medicine's gnotobiotic mouse facility. Altered Schaedler Flora (ASF) mice were generated by colonizing GF mice with the defined ASF community[41] and allowing 5 generations of breeding before use.

The investigators were not blinded to the conditions of the experiments during data collection and analysis.

Fungal Strains and Lysates Preparation

Candida albicans SC5314 (ATCC® MYA-2876™), *Saccharomyces cerevisiae* (ATCC® MYA-796™), *Aspergillus amstelodami* (ATCC® 46362™), and *Wallemia sebi* (ATCC® 42964™) were obtained from the American Type Culture Collection (Manassas, VA,

supplementary Table S1). *Saccharomycopsis fibuligera* was isolated from murine fecal material (supplementary Table S1). Ca-dREP, a *C. albicans* strains that emits green fluorescence in the yeast phase and red fluorescence in the hyphal phase was constructed as follows. The promoter of *HWP1*, a hyphal specifically expressed adhesin of *C. albicans*[79], was amplified from the SC5314 genome[80] using primers pHWP1-up (ACGTTCTAGATTATCGGGTGATTAATAACATGCTGC) and pHWP1-lo (ACGTCTCGAGATTGACGAAACTAAAAGCGAGTGAC) that incorporate at their 5' end restriction sites for XbaI and XhoI respectively (underlined in the primers sequence). The 2084 bp amplified fragment was purified and after digestion with the indicated enzymes, cloned in a SpeI and SalI digested plasmid pASM0-RFP, generating pASM10-RFP. pASM0-RFP is a *C. albicans* integrative plasmid expressing a *C. albicans* optimized RFP[81] under the control of the TET^{OFF} promoter[82]. pASM10-RFP plasmid was digested with the restriction enzymes KpnI and SacII and used to transform strain SN100 (*his1Δ/his1Δ URA3/ura3Δ::imm434 IRO1/iro1Δ::imm434*)[83] using electroporation, forcing recombination at the *ADH1* genomic region. Transformants were selected on YPD plates supplemented with 200 μg/mL nourseothricin sulphate. The proper integration of the construction was checked using primers upstream the *HWP1* promoter and within the inserted construction as well as by examination of red fluorescence in cells triggered by filamentation. This intermediate was named ERG1390. We then used the *YWP1* gene[84] to develop a yeast-phase specific reporter. We first amplified the *YWP1* promoter from the SC5314 strain using primers pYWP1-up (ACGTGGATCCCCATCATTTATTTCATCTTGGAAATG) and pYWP1-lo (ACGTGTCGACTATTATTATTATTTCTTGGATTTGATAAATTAAT) that include at the 5' restriction sites for BamHI and SalI respectively (underlined in the primers sequence). The 2198 amplified fragment was digested with BamHI and SalI and cloned in a BamHI and SalI digested pDH0M-GFP[85], an integrative plasmid vector that uses *HIS1* as genetic marker allowing integration of any promoter upstream GFP. The resulting plasmid, pDHM11-GFP was digested with KpnI and SacI and used to transform intermediate ERG1390, directing the construction to the *ARD1* genomic region using the same transformation protocol as indicated above and minimal (His-) medium plates giving rise of the *C. albicans* double reporter Ca-dREP.

WT *C. albicans* reporter strain CAF2-RFP that constitutively expresses RFP was generated by replacement of the 5' *ADH1* XbaI - SacII region of pNIM1R-GFP with a 1630 bp region derived from pNIMX[86] that comprises the *C. albicans TDH3* promoter. Yeast-locked reporter *cph1Δ/Δ efg1Δ/Δ* GFP strain was constructed inserting a fragment carrying the GFP under the TET^{OFF} promoter derived from KpnI and KspI restriction enzyme digest of plasmid pNIM1R-GFP[81] to force recombination at the *ADH1* region on a URA+ derivative of strain HLC69 (*cph1Δ/Δ efg1Δ/Δ ura3Δ/Δ*)[49] which was constructed by integration of pRM1 plasmid[87] at the *LEU2* genomic region. *C. albicans* ece1Δ/Δ and parental strains were generated as previously described[65].

All fungi were cultured in aerobic conditions overnight in Sabouraud Dextrose Broth (SDB; EMD Chemicals) at 37°C. In experiment where lysates from yeast-locked strain were used, $efg1^{\Delta/\Delta}cph1^{\Delta/\Delta}$ and WT *C. albicans* strains were cultured under hyphae-inducing conditions using GlcNAc supplemented media[88]. For fungal lysate preparation, fungal cultures were fixed in 4% paraformaldehyde for 60 minutes at 4°C. Fungal suspensions were washed 3

times by pelleting at 900 × g for 2 minutes, aspirating the supernatant, and resuspending the pellet in molecular-grade water. Fungi were treated with three freeze-thaw cycles of 10 minutes in dry ice, then 10 minutes in a 75°C incubator. Finally, fungal suspensions were sonicated for eight cycles of 15 seconds on/30 seconds off. Fungal debris was centrifuged at 4000 rpm for 2 minutes, after which supernatant was used for ELISA plate coating.

Fecal and Mucosal Washings' Samples Flow Cytometry-based Analysis

Age and sex information for human samples assessed in this study can be found in supplementary Table S2. For assessments of the sIgA-bound fractions of murine fecal and human fecal or mucosal lavage samples by flow cytometry, samples were collected from 7–8-week-old mice or healthy human individuals and homogenized in sterile PBS at 25mg/mL and filtered through a 70μm strainer-capped tube (Falcon, 5mL). C57/BL6 WT mice born in our facility (WCM-CE)[29,34] were used for the assessment of sIgA bounding to native mycobiota while C57BL/6J WT mice raised in the Jackson Laboratory (JAX) were used in Ca-dREP colonization studies. Size separation was achieved by centrifugation at 900 × g for 10 minutes. The resulting large (fungal) and small (bacterial) fractions were used for applications such as flow cytometry analysis and/or sorting and/or DNA isolation. After samples were blocked for 30 minutes with staining buffer (2% BSA/ 0.05% sodium azide), mouse samples were stained with 1:500 mIgA-PE (Thermofisher), 1:200 mIgG-AF647 (Jackson Immunoresearch), or 1:200 mIgM-PE-Cy7 (eBioscience™) antibodies for 45 minutes at 4°C. Human samples were similarly blocked and stained with 1:400 hIgA-PE (Miltenyi) and 1:400 hIgG-AF647 (Southern Biotech) antibodies. To avoid spectral overlap between PE antibodies and RFP^+ Ca-dREP or CAF2-RFP, sIgA binding assays involving these strains replaced used APC-labeled mIgA (Thermofisher) and hIgA (Miltenyi) secondary antibodies instead of PE-labeled, with the same clones at the same concentration. Stained feces were then fixed in 4% formalin, followed by staining with 1:1000 SYBR-Green I (Invitrogen)/1:500 calcofluor white (Sigma).

Antifungal ELISA Assay

For assessment of free sIgA titers in human mucosal lavage samples or mouse fecal pellets, samples were diluted, homogenized and centrifuged at 8000 × g for 10 minutes. The resulting supernatant was weighted, resuspended to 100μg material/μL with sterile PBS containing protease inhibitor (Sigma) and used in our assays.

Total levels and antifungal titers of sIgA in mouse and human feces or mucosal washings were measured by enzyme-linked immunosorbent assay (ELISA). 96-well high-binding polystyrene plates (Corning) were coated with 50μL per well. Total free sIgA was assessed with anti-mouse-IgG-IgA-IgM (Sigma) or anti-human Ig (Southern) diluted 1:2000 in coating buffer (50mM carbonate-bicarbonate buffer, pH 9.5). Fungal lysates prepared as described above were diluted 1:50 in coating buffer. *Saccharomyces cerevisiae* mannan (Sigma), bacterial flagellin from *S. typhimurium* (Invivogen), Ece1-III (candidalysin) and Sap6 (MyBioSource) were coated at 2μg/mL in buffer, respectively. For total IgA analyses in mouse and human feces or mucosal washings, sIgA-containing supernatant was diluted 250X and 4000X in 0.5% BSA, and 50μL suspension were applied per well. After total IgA measurements, antigen-specific IgA was similarly plated with 50μL after normalizing

total IgA concentrations between all samples. Total IgA titers were measured against serial dilution standards of mouse (Bethyl Laboratories) and human (Southern) unconjugated IgA antibodies. After overnight incubation at 4°C, plates were washed and incubated for 1 hour at room temperature with 1000X goat anti-human or anti-mouse IgA-HRP or IgG-HRP antibodies (Southern). Plates were washed, followed by development with TMB HRP substrate (BD Biosciences) and quenched with 0.36M H_2SO_4. Plates were measured at OD 450nm on a microtiter plate reader (Menlo Park, CA).

Cell processing, Flow Cytometry, Fungal cell sorting, Imaging and Antibodies

Cell suspensions prepared as described above were blocked with CD16/CD32 (Mouse BD Fc Block™, 2.4G2, BD Biosciences). For B cell compartment analysis, suspensions were stained with antibodies (supplementary Table S1) against CD45-BV650 (30-F11, Tonbo), CD4 (GK1.5, eBioscience), B220 (RA3-B62, Biolegend), IgA (PE, mA-6E1, eBioscience), IgM (FITC, II/41, Thermofisher), Fas (alternatively named CD95, Jo2, BD Pharmingen), and GL7 antigen (GL7, Biolegend). Dead cells were excluded with eBioscience Fixable Viability Dye eFluor 455UV (Thermofisher). In phagocyte depletion experiments, suspensions were stained with antibodies against CD45 (30-F11, Tonbo), I-A/I-E a (M5/114.15.2, Biolegend), CD11c (N418, Biolegend), CD11b (M1/70, Thermofisher), CX3CR1 (SA011F11, Biolegend), and CD103 (2E7, Thermofisher). Dead cells were excluded with eBioscience Fixable Viability Dye eFluor 506 (Thermofisher). Flow cytometry was performed using a LSRFortessa (BD Biosciences) and data were analyzed with FlowJo V10 software (TreeStar). Images were acquired under an inverted Nikon Eclipse Ti microscope (Nikon).

CFW^+ GFP^+ Ca-dREP was sorted on FACSAria III (BD Bioscience, with a 100μm flow cell) from mouse fecal samples into IgA^+ and IgA^- populations and examined under an inverted Nikon Eclipse Ti microscope (Nikon). For morphology evaluation studies based on SSC and FSC, IgA^+ CFW^+GFP^+ Ca-dREP and $IgA^-CFW^+GFP^+$ Ca-dREP were sorted on FACSAria III mouse fecal samples into an SSC^{hi} FSC^{hi} and SSC^{lo} FSC^{lo} populations and examined under an inverted Nikon Eclipse Ti microscope (Nikon).

In vivo Models of Intestinal Fungal Colonization

For monocolonization of GF and ASF mice, 7–8-week-old mice were orally gavaged with 1×10^8 fungal cells cultured from pure isolates grown overnight at 37°C. Fecal sIgA assessment was conducted at indicated time points and tissue harvesting for B cell compartment and staining was conducted after two weeks. For colonization of SPF mice, oral gavage of 7–8-week-old mice occurred two days after administering 0.4g/L cefoperazone *ad libitum* and continued throughout the entirety of the experiment.

Isolation of Peyer's patches (PP) and colonic lamina propria (cLP)

Four to six PP were excised from the ileum of each mouse. Colons were isolated, opened longitudinally, washed of fecal contents and then cut into pieces. Such obtained tissues were placed into Hank's Balanced Salt Solution (HBSS) medium (Thermofisher), supplemented with 2 mM EDTA, and were shaken for 10 min at 37°C, followed washing and mincing in a medium consisting of RPMI 1640 (Thermofisher), 5% FBS, 0.5 mg/ml collagenase

type VIII (Sigma), 5 U/ml DNase (Roche Diagnostics), 100 IU/ml penicillin and 100 μg/ml streptomycin (Thermofisher) and filtered through a nylon mesh (70μm). Processed tissues were once again filtered through mesh, washed twice in PBS, and resuspended in cold PBS supplemented with 2% BSA for antibody staining.

In vitro Antifungal IgA Binding Assay

For assessment of free sIgA binding to *C. albicans*, human mucosal lavage samples, human fecal samples or mouse fecal pellets were used as a source of sIgA. Samples were diluted, homogenized and centrifuged at 8000 × g for 10 minutes. The resulting supernatant was separated from solid pelleted material, sterilized by passage through a 0.2μm filter, and resuspended to 100μg material/μL with sterile PBS containing protease inhibitor (Sigma). The resulting material was used for staining of Ca-dREP previously grown under hyphae inducing conditions and incubated with staining buffer (2% BSA/0.05% sodium azide) for 30 minutes. Samples ware then washed and stained with anti-human or anti-mouse IgA respectively, followed by fixation in 4% formalin (for microscopy evaluation) or in 1% PFA/0.05% sodium azide, containing buffer (for flow cytometry).

In vitro two partner assay for hyphal morphogenesis assessment in the presence of human sIgA.

sIgA from human fecal samples prepared as described above was isolated using Peptide M Agarose (InvivoGen) loaded into G-Trap FPLC columns (G-Biosciences). Pooled and purified IgA was then desalted through buffer exchange to PBS using Amicon® Ultra-15 Centrifugal filter tubes (Milipore) for dilution used in the assay. Caco2 cells (ATCC) were seeded into 24-well tissue culture treated plates at a concentration of 0.2×10^5/ml in DMEM Medium (10% fetal bovine serum, 1% GlutaMAX solution (gibco), 1% penicillin/streptomycin solution, Corning) for 3 days at 37 °C. Each well was co-incubated with live Ca-dREP at MOI 1 in DMEM Medium (serum free, 1% penicillin/streptomycin solution) and supplemented with 5μg sIgA per well at 0 and 6 hours. The assay was terminated at 24 hours (used as the last time point). Samples were collected at indicated time points and fungal morphology was assessed by flow cytometry using the in vitro antifungal IgA binding assay as described above.

Quantification and statistical analysis.

All flow cytometry data were collected by FACSDiva Software (v9.0). Statistics were computed using GraphPad Prism version 8 (GraphPad Software). Statistical details of experiments are reported in the figure legends. The P value(s) reported in the figure legends are the likelihood(s) of observing the effect size(s) if the null hypothesis of zero difference is true. All statistical tests represented are two-sided analyses. Besides two mice from the experiment in Fig. 3h–k (referenced in figure legend), no mice were excluded from our analyses. Normal distribution was not assumed in the statistical analyses shown in this study, and exact *P* values of these analyses are shown on each graph separately. $P < 0.05$ is considered statistically significant.

Extended Data

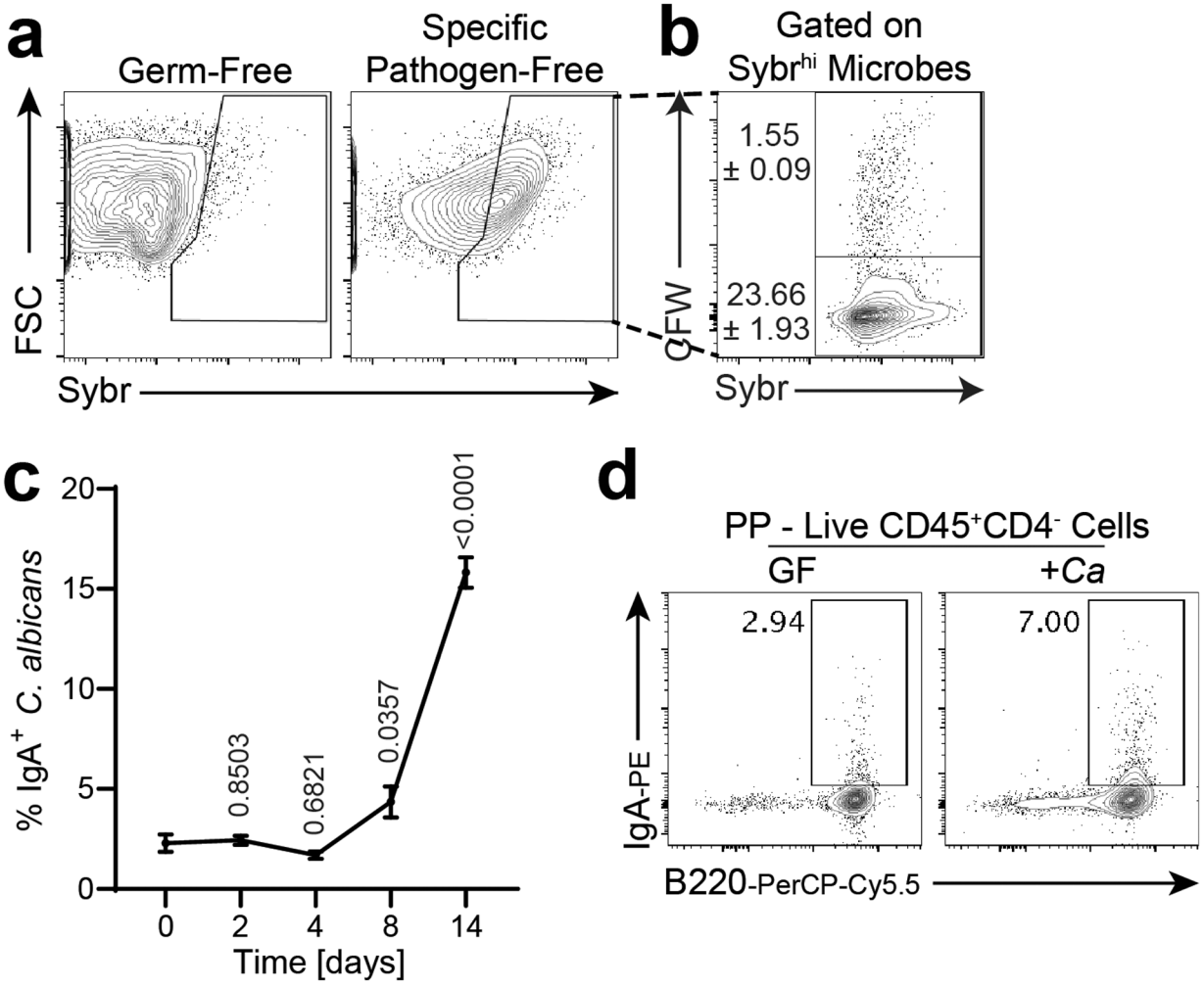

Extended Data Fig. 1. Identification of gut fungi from fecal material by flow cytometry and anti-*C. albicans* sIgA dynamics.

a, Microbes in fecal material from SPF WT WCM-CE mice were distinguished as a $Sybr^{hi}$ population that is absent in GF mouse feces. **b,** Fungi ($Sybr^{hi}CFW^{+}$) were enriched from bacteria ($Sybr^{hi}CFW^{-}$) through size separation by 900 × g centrifugation and calcofluor white (CFW) staining of the resulting pellet. **c,** *C. albicans* cultured for 18 hours in hyphae-inductive media was stained with fecal supernatant from *C. albicans*-colonized GF mice ($N = 6$) collected at 0, 2-, 4-, 8- and 14-days post colonization, followed by sIgA staining. Analysis of IgA binding representative of two independent experiments, one-way ANOVA, followed by Sidak's test. **d**, Representative flow cytometry plots of frequency of $B220^{+}IgA^{+}$ among Live $CD45^{+}CD4^{-}$ cells in the PP of germ-free (GF) mice orally gavaged with PBS (GF) or colonized for two weeks with *C. albicans* (+*Ca*). Data in (c) represents mean ± SEM.

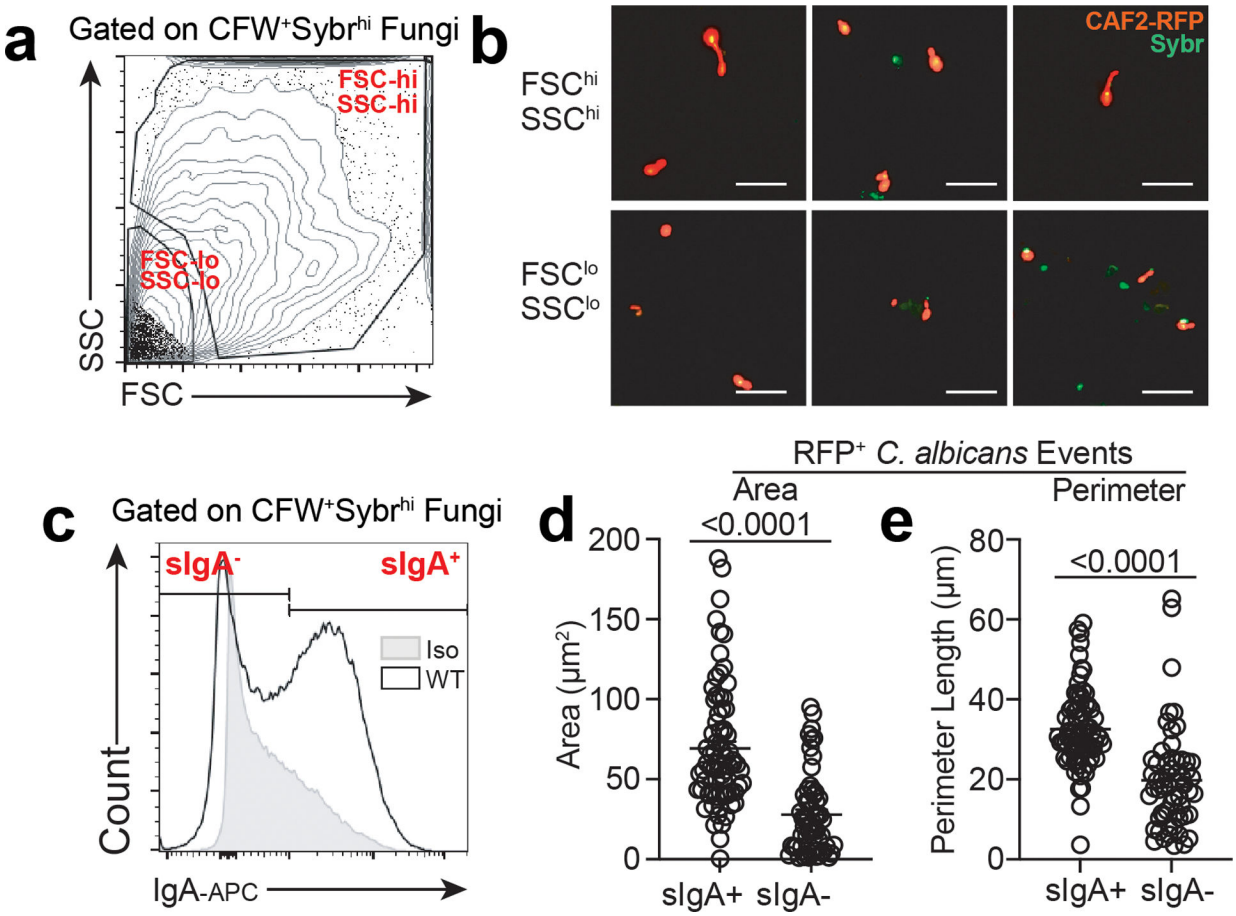

Extended Data Fig. 2. CFW^{+}Sybr^{hi} FSC^{hi}SSC^{hi} *C. albicans* population in feces represents hyphal/pseudohyphal fungal morphologies that are preferentially bound by sIgA.

a, CFW^{+}Sybr^{hi} fungal population from feces of SPF mice colonized with CAF2-RFP *C. albicans* was sorted into FSC^{hi}SSC^{hi} and FSC^{lo}SSC^{lo} fractions. Constitutive expression of RFP in this strain allows for high visibility and resistance to signal quenching upon prolonged light exposure during flow cytometry and microscopy on the same material. **b,** Immunofluorescence microscopy of sorted material from (a). Composite images at 20X magnification of FSC^{hi}SSC^{hi} and FSC^{lo}SSC^{lo} shown in left and right panels, respectively. Scale bar represents 25μm. Data representative of two independent experiments. **c,** CFW^{+}Sybr^{hi} fungal population from feces of SPF mice colonized with CAF2-RFP was sorted into IgA^{+} and IgA^{-} populations. Gray histograms represent IgA-isotype control staining used to distinguish sorted populations. **d-e,** Area (d) and perimeter length (e) of CAF2-RFP were compared between IgA^{+} and IgA^{-} sorted populations. Data represents two independent experiments, mean ± SEM. Two-sided Mann-Whitney test. $N = 5$.

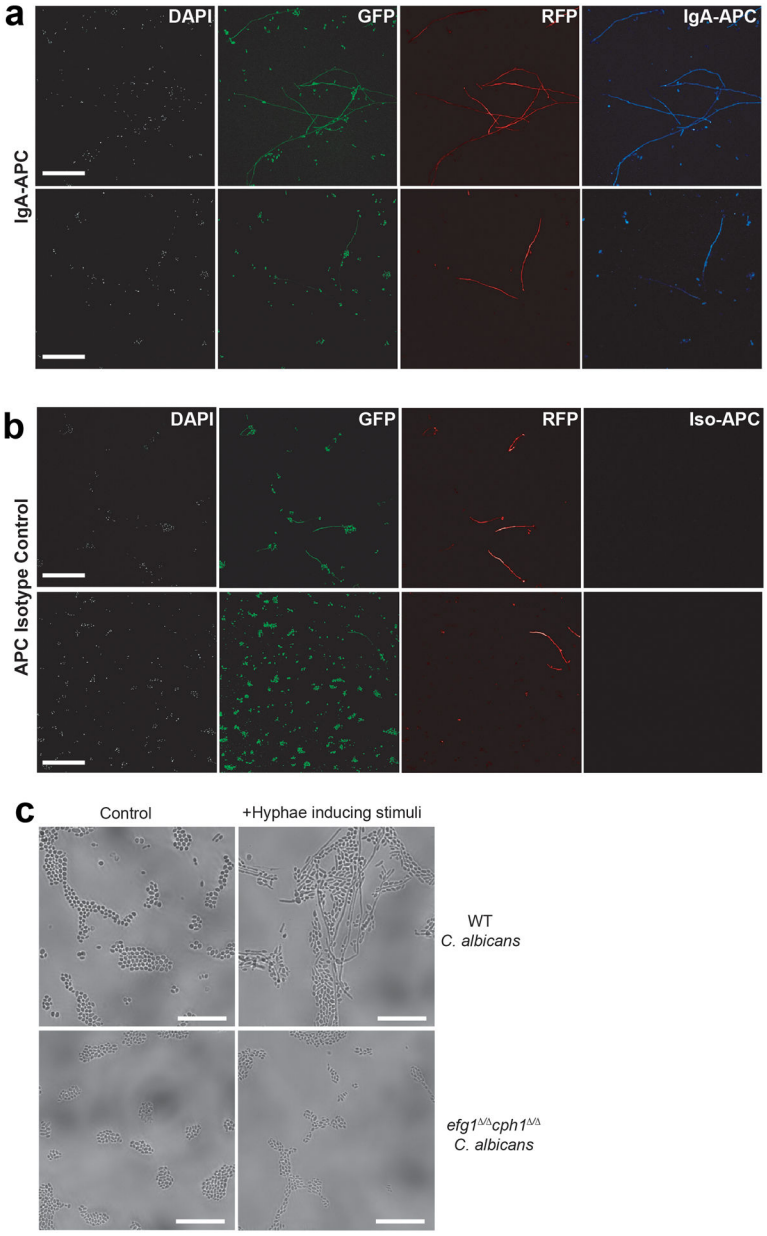

Extended Data Fig. 3. Assessment of Ca-dREP *C. albicans* double reporter strain upon IgA staining and hyphae forming deficiency of *efg1Δ/Δ cph1Δ/Δ C. albicans* strain.

a-b, Immunofluorescence microscopy of Ca-dREP incubated with human fecal supernatant as a source of sIgA and stained with DAPI and anti-human IgA-APC (a) or an APC isotype control (b). Single channel staining of 2 samples shown. Left to right: DAPI, constitutive *ENO1*-GFP expression, hyphae-specific *HWP1*-RFP expression, and anti-human IgA-APC (a) or APC isotype control (b). Top rows in **a** and **b** correspond to composite images in Fig. 2d–e, representing three independent experiments. Scale bar represents 50μm**. c**, Hyphae-competent (WT), but not hyphae-deficient (yeast-locked; *efg1Δ/Δ cph1Δ/Δ*) strains of *C. albicans* forms hyphae upon hyphae-inducing stimuli *in vitro*. Scale bar represents 25μm.

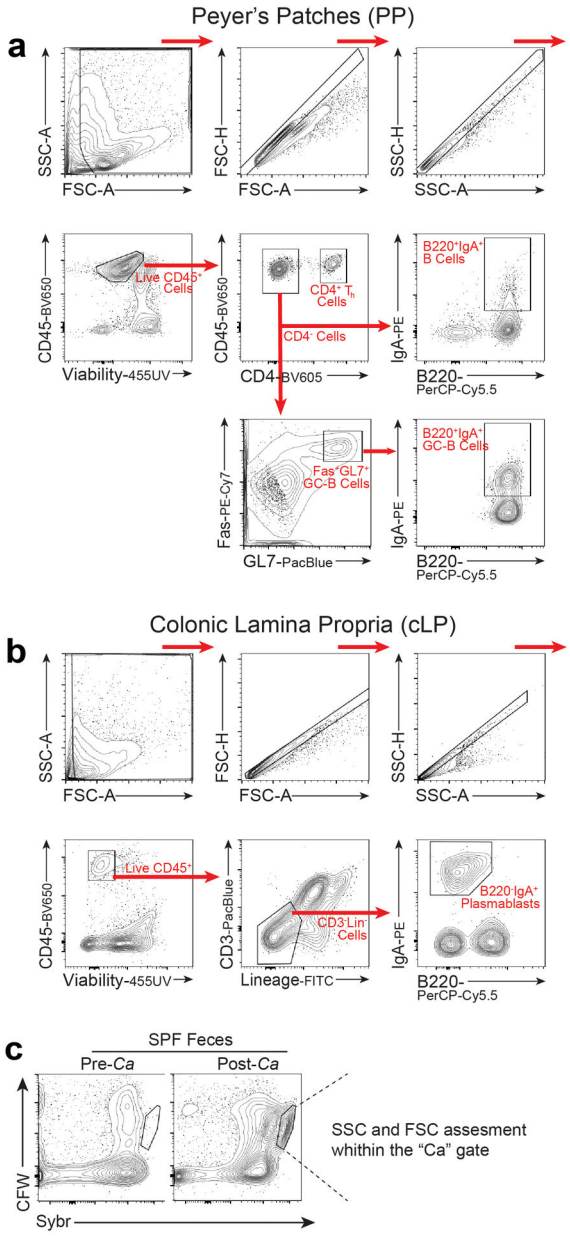

Extended Data Fig. 4. Flow cytometry gating strategy in PPs, LP and in feces.

a-b, Cell gating startegy for assessment of IgA^+ GC B cell in PPs (a) and IgA^+ plasmablasts in lamina propria (b). **c**, gating strategy of *C.albicans* cells in feces pre- and post- *C.albicans* (C.a) colonization.

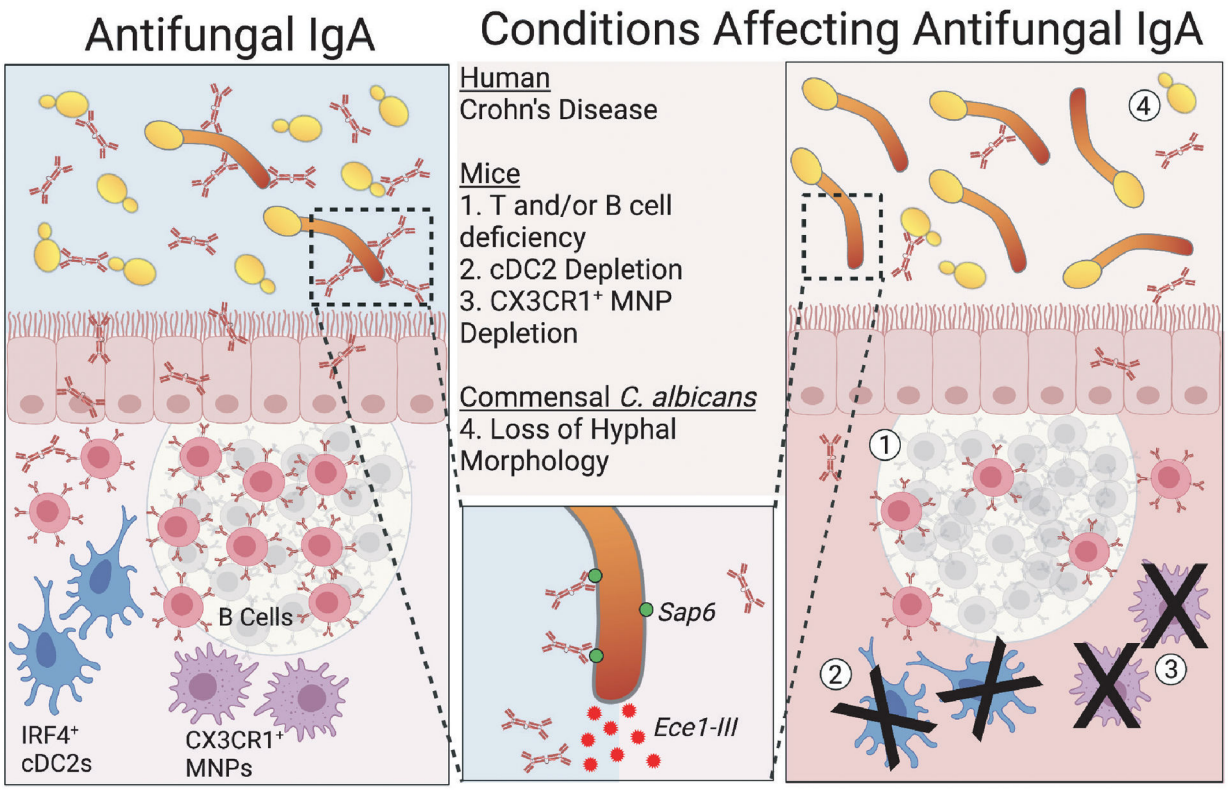

Extended Data Fig. 5. Graphical abstract for the model of antifungal IgA induction by and regulation of intestinal fungal commensalism.
(Credit: Created with BioRender.com)

Supplementary Material

Refer to Web version on PubMed Central for supplementary material.

Acknowledgments

We thank members of the Iliev laboratory for their critical reviews of the manuscript. We thank Ramnik Xavier for discussion and for providing analysis that helped us with shaping the hypothesis. We thank all contributing members of the JRI IBD Live Cell Bank Consortium, and the Microbiome Core Laboratory of Weill Cornell Medicine. Support for human sample acquisition through the JRI IBD Live Cell Bank is provided by the JRI, Jill Roberts Center for IBD, Cure for IBD, the Rosanne H. Silbermann Foundation and Weill Cornell Medicine Division of Pediatric Gastroenterology and Nutrition. JP and ER were funded by PGC2018–095047-B-I00 from MINECO and InGEMICS (B2017/BMD¬3691) from CAM. Research in the Iliev laboratory is supported by US National Institutes of Health (R01AI163007, R01DK113136 and R01DK121977), the Leona M. and Harry B. Helmsley Charitable Trust, the Irma T. Hirschl Career Scientist Award, Crohn's and Colitis Foundation, Pilot Project Funding from the Center for Advanced Digestive Care (CADC) and the Burrough Welcome Trust PATH Award.

Data availability.

The data that support the findings of this study are available from the corresponding author upon request.

References:

1. Hapfelmeier S, et al. Reversible microbial colonization of germ-free mice reveals the dynamics of IgA immune responses. Science 328, 1705–1709 (2010). [PubMed: 20576892]
2. Slack E, et al. Innate and Adaptive Immunity Cooperate Flexibly to Maintain Host-Microbiota Mutualism. Science 325, 617 (2009). [PubMed: 19644121]
3. Cerutti A & Rescigno M The Biology of Intestinal Immunoglobulin A Responses. Immunity 28, 740–750 (2008). [PubMed: 18549797]
4. Pabst O & Slack E IgA and the intestinal microbiota: the importance of being specific. Mucosal Immunology 13, 12–21 (2020). [PubMed: 31740744]
5. Spencer J & Sollid LM The human intestinal B-cell response. Mucosal Immunology 9, 1113–1124 (2016). [PubMed: 27461177]
6. Bunker JJ & Bendelac A IgA Responses to Microbiota. Immunity 49, 211–224 (2018). [PubMed: 30134201]
7. Bunker JJ, et al. Natural polyreactive IgA antibodies coat the intestinal microbiota. Science 358, eaan6619 (2017). [PubMed: 28971969]
8. Bunker JJ, et al. Innate and Adaptive Humoral Responses Coat Distinct Commensal Bacteria with Immunoglobulin A. Immunity 43, 541–553 (2015). [PubMed: 26320660]
9. Uchimura Y, et al. Antibodies Set Boundaries Limiting Microbial Metabolite Penetration and the Resultant Mammalian Host Response. Immunity 49, 545–559.e545 (2018). [PubMed: 30193848]
10. Geuking MB, et al. Intestinal bacterial colonization induces mutualistic regulatory T cell responses. Immunity 34, 794–806 (2011). [PubMed: 21596591]
11. Macpherson AJ, et al. IgA production without mu or delta chain expression in developing B cells. Nat Immunol 2, 625–631 (2001). [PubMed: 11429547]
12. Gopalakrishna KP, et al. Maternal IgA protects against the development of necrotizing enterocolitis in preterm infants. Nature Medicine 25, 1110–1115 (2019).
13. Nowosad CR, et al. Tunable dynamics of B cell selection in gut germinal centres. Nature 588, 321–326 (2020). [PubMed: 33116306]
14. Chen H, et al. BCR selection and affinity maturation in Peyer's patch germinal centres. Nature 582, 421–425 (2020). [PubMed: 32499646]
15. Kabbert J, et al. High microbiota reactivity of adult human intestinal IgA requires somatic mutations. Journal of Experimental Medicine 217(2020).
16. Palm NW, et al. Immunoglobulin A coating identifies colitogenic bacteria in inflammatory bowel disease. Cell 158, 1000–1010 (2014). [PubMed: 25171403]
17. Viladomiu M, et al. IgA-coated *E. coli* enriched in Crohn's disease spondyloarthritis promote T_H17-dependent inflammation. Science Translational Medicine 9, eaaf9655 (2017). [PubMed: 28179509]
18. Sokol H, et al. Fungal microbiota dysbiosis in IBD. Gut 66, 1039–1048 (2017). [PubMed: 26843508]
19. Liguori G, et al. Fungal Dysbiosis in Mucosa-associated Microbiota of Crohn's Disease Patients. Journal of Crohn's and Colitis 10, 296–305 (2015).
20. Lewis JD, et al. Inflammation, Antibiotics, and Diet as Environmental Stressors of the Gut Microbiome in Pediatric Crohn's Disease. Cell Host Microbe 18, 489–500 (2015). [PubMed: 26468751]
21. Hoarau G, et al. Bacteriome and Mycobiome Interactions Underscore Microbial Dysbiosis in Familial Crohn's Disease. mBio 7(2016).
22. Limon JJ, et al. Malassezia Is Associated with Crohn's Disease and Exacerbates Colitis in Mouse Models. Cell Host Microbe 25, 377–388.e376 (2019). [PubMed: 30850233]
23. Leonardi I, et al. Fungal Trans-kingdom Dynamics Linked to Responsiveness to Fecal Microbiota Transplantation (FMT) Therapy in Ulcerative Colitis. Cell host & microbe 27, 823–829 e823 (2020). [PubMed: 32298656]
24. Leonardi I, et al. CX3CR1(+) mononuclear phagocytes control immunity to intestinal fungi. Science 359, 232–236 (2018). [PubMed: 29326275]

25. Jain U, et al. Debaryomyces is enriched in Crohn's disease intestinal tissue and impairs healing in mice. Science 371, 1154–1159 (2021). [PubMed: 33707263]
26. Yang AM, et al. Intestinal fungi contribute to development of alcoholic liver disease. J Clin Invest 127, 2829–2841 (2017). [PubMed: 28530644]
27. Israeli E, et al. Anti-Saccharomyces cerevisiae and antineutrophil cytoplasmic antibodies as predictors of inflammatory bowel disease. Gut 54, 1232–1236 (2005). [PubMed: 16099791]
28. Standaert-Vitse A, et al. Candida albicans colonization and ASCA in familial Crohn's disease. Am J Gastroenterol 104, 1745–1753 (2009). [PubMed: 19471251]
29. Doron I, et al. Human gut mycobiota tune immunity via CARD9-dependent induction of anti-fungal IgG antibodies. Cell 184, 1017–1031.e1014 (2021). [PubMed: 33548172]
30. Millet N, Solis NV & Swidergall M Mucosal IgA Prevents Commensal Candida albicans Dysbiosis in the Oral Cavity. Frontiers in Immunology 11(2020).
31. Witchley JN, et al. Candida albicans Morphogenesis Programs Control the Balance between Gut Commensalism and Invasive Infection. Cell host & microbe 25, 432–443 e436 (2019). [PubMed: 30870623]
32. Liang S-H, et al. Hemizygosity Enables a Mutational Transition Governing Fungal Virulence and Commensalism. Cell Host & Microbe 25, 418–431.e416 (2019). [PubMed: 30824263]
33. Gow NAR & Hube B Importance of the Candida albicans cell wall during commensalism and infection. Current Opinion in Microbiology 15, 406–412 (2012). [PubMed: 22609181]
34. Doron I, Leonardi I & Iliev ID Profound mycobiome differences between segregated mouse colonies do not influence Th17 responses to a newly introduced gut fungal commensal. Fungal Genet Biol 127, 45–49 (2019). [PubMed: 30849443]
35. Koch Meghan A., et al. Maternal IgG and IgA Antibodies Dampen Mucosal T Helper Cell Responses in Early Life. Cell 165, 827–841 (2016). [PubMed: 27153495]
36. Macpherson AJ, et al. A primitive T cell-independent mechanism of intestinal mucosal IgA responses to commensal bacteria. Science 288, 2222–2226 (2000). [PubMed: 10864873]
37. Smith K, McCoy KD & Macpherson AJ Use of axenic animals in studying the adaptation of mammals to their commensal intestinal microbiota. Seminars in Immunology 19, 59–69 (2007). [PubMed: 17118672]
38. Senda S, Cheng E & Kawanishi H Aging-Associated Changes in Murine Intestinal Immunoglobulin A and M Secretions. Scandinavian Journal of Immunology 27, 157–164 (1988). [PubMed: 3340826]
39. Lécuyer E, et al. Segmented filamentous bacterium uses secondary and tertiary lymphoid tissues to induce gut IgA and specific T helper 17 cell responses. Immunity 40, 608–620 (2014). [PubMed: 24745335]
40. Fan D, et al. Activation of HIF-1α and LL-37 by commensal bacteria inhibits Candida albicans colonization. Nat Med 21, 808–814 (2015). [PubMed: 26053625]
41. Zhai B, et al. High-resolution mycobiota analysis reveals dynamic intestinal translocation preceding invasive candidiasis. Nature Medicine 26, 59–64 (2020).
42. Li X, et al. Response to Fungal Dysbiosis by Gut-Resident CX3CR1(+) Mononuclear Phagocytes Aggravates Allergic Airway Disease. Cell Host Microbe 24, 847–856.e844 (2018). [PubMed: 30503509]
43. Schaedler RW, Dubs R & Costello R ASSOCIATION OF GERMFREE MICE WITH BACTERIA ISOLATED FROM NORMAL MICE. J Exp Med 122, 77–82 (1965). [PubMed: 14325475]
44. Tso GHW, et al. Experimental evolution of a fungal pathogen into a gut symbiont. Science 362, 589 (2018). [PubMed: 30385579]
45. Pande K, Chen C & Noble SM Passage through the mammalian gut triggers a phenotypic switch that promotes Candida albicans commensalism. Nature Genetics 45, 1088–1091 (2013). [PubMed: 23892606]
46. Pierce JV, Dignard D, Whiteway M & Kumamoto CA Normal Adaptation of *Candida albicans* to the Murine Gastrointestinal Tract Requires Efg1p-Dependent Regulation of Metabolic and Host Defense Genes. Eukaryotic Cell 12, 37 (2013). [PubMed: 23125349]

47. Pierce JV & Kumamoto CA Variation in *Candida albicans EFG1* Expression Enables Host-Dependent Changes in Colonizing Fungal Populations. mBio 3, e00117–00112 (2012). [PubMed: 22829676]
48. Allert S, et al. Candida albicans-Induced Epithelial Damage Mediates Translocation through Intestinal Barriers. mBio 9, e00915–00918 (2018). [PubMed: 29871918]
49. Lo HJ, et al. Nonfilamentous C. albicans mutants are avirulent. Cell 90, 939–949 (1997). [PubMed: 9298905]
50. Hube B From commensal to pathogen: stage- and tissue-specific gene expression of Candida albicans. Curr Opin Microbiol 7, 336–341 (2004). [PubMed: 15288621]
51. Mowat AM & Agace WW Regional specialization within the intestinal immune system. Nature Reviews Immunology 14, 667–685 (2014).
52. Koscsó B, et al. Gut-resident CX3CR1^{hi} macrophages induce tertiary lymphoid structures and IgA response in situ. Science Immunology 5, eaax0062 (2020). [PubMed: 32276965]
53. Farache J, Zigmond E, Shakhar G & Jung S Contributions of dendritic cells and macrophages to intestinal homeostasis and immune defense. Immunol Cell Biol 91, 232–239 (2013). [PubMed: 23399695]
54. Bogunovic M, Mortha A, Muller PA & Merad M Mononuclear phagocyte diversity in the intestine. Immunol Res 54, 37–49 (2012). [PubMed: 22562804]
55. Chikina AS, et al. Macrophages Maintain Epithelium Integrity by Limiting Fungal Product Absorption. Cell 183, 411–428.e416 (2020). [PubMed: 32970988]
56. Schulz O, et al. Intestinal CD103+, but not CX3CR1+, antigen sampling cells migrate in lymph and serve classical dendritic cell functions. Journal of Experimental Medicine 206, 3101–3114 (2009).
57. Joeris T, Müller-Luda K, Agace WW & Mowat AM Diversity and functions of intestinal mononuclear phagocytes. Mucosal Immunology 10, 845–864 (2017). [PubMed: 28378807]
58. Kubinak Jason L., et al. MyD88 Signaling in T Cells Directs IgA-Mediated Control of the Microbiota to Promote Health. Cell Host & Microbe 17, 153–163 (2015). [PubMed: 25620548]
59. Macpherson AJ, McCoy KD, Johansen FE & Brandtzaeg P The immune geography of IgA induction and function. Mucosal Immunology 1, 11–22 (2008). [PubMed: 19079156]
60. Chen K, Magri G, Grasset EK & Cerutti A Rethinking mucosal antibody responses: IgM, IgG and IgD join IgA. Nature Reviews Immunology 20, 427–441 (2020).
61. Ha S.-a., et al. Regulation of B1 cell migration by signals through Toll-like receptors. Journal of Experimental Medicine 203, 2541–2550 (2006).
62. Netea MG, Joosten LAB, van der Meer JWM, Kullberg B-J & van de Veerdonk FL Immune defence against Candida fungal infections. Nature Reviews Immunology 15, 630–642 (2015).
63. Li XV, Leonardi I & Iliev ID Gut Mycobiota in Immunity and Inflammatory Disease. Immunity 50, 1365–1379 (2019). [PubMed: 31216461]
64. Liu Y & Filler SG Candida albicans Als3, a multifunctional adhesin and invasin. Eukaryotic cell 10, 168–173 (2011). [PubMed: 21115738]
65. Moyes DL, et al. Candidalysin is a fungal peptide toxin critical for mucosal infection. Nature 532, 64–68 (2016). [PubMed: 27027296]
66. Fransen F, et al. BALB/c and C57BL/6 Mice Differ in Polyreactive IgA Abundance, which Impacts the Generation of Antigen-Specific IgA and Microbiota Diversity. Immunity 43, 527–540 (2015). [PubMed: 26362264]
67. Peterson DA, McNulty NP, Guruge JL & Gordon JI IgA response to symbiotic bacteria as a mediator of gut homeostasis. Cell Host Microbe 2, 328–339 (2007). [PubMed: 18005754]
68. Shimoda M, Inoue Y, Azuma N & Kanno C Natural polyreactive immunoglobulin A antibodies produced in mouse Peyer's patches. Immunology 97, 9–17 (1999). [PubMed: 10447709]
69. Brand A Hyphal growth in human fungal pathogens and its role in virulence. Int J Microbiol 2012, 517529 (2012). [PubMed: 22121367]
70. Wu G, et al. Genus-Wide Comparative Genomics of Malassezia Delineates Its Phylogeny, Physiology, and Niche Adaptation on Human Skin. PLOS Genetics 11, e1005614 (2015). [PubMed: 26539826]

71. Saadatzadeh MR, Ashbee HR, Holland KT & Ingham E Production of the mycelial phase of Malassezia in vitro. Medical Mycology 39, 487–493 (2001). [PubMed: 11798054]
72. Loures FV, et al. Recognition of Aspergillus fumigatus hyphae by human plasmacytoid dendritic cells is mediated by dectin-2 and results in formation of extracellular traps. PLoS Pathog 11, e1004643 (2015). [PubMed: 25659141]
73. Moyes DL, et al. Candida albicans yeast and hyphae are discriminated by MAPK signaling in vaginal epithelial cells. PLoS One 6, e26580 (2011). [PubMed: 22087232]
74. Zuza-Alves DL, Silva-Rocha WP & Chaves GM An Update on Candida tropicalis Based on Basic and Clinical Approaches. Front Microbiol 8, 1927–1927 (2017). [PubMed: 29081766]
75. Gantner BN, Simmons RM & Underhill DM Dectin-1 mediates macrophage recognition of Candida albicans yeast but not filaments. Embo j 24, 1277–1286 (2005). [PubMed: 15729357]
76. Lin X, Alspaugh JA, Liu H & Harris S Fungal morphogenesis. Cold Spring Harb Perspect Med 5, a019679–a019679 (2014). [PubMed: 25367976]
77. McKenzie CG, et al. Contribution of Candida albicans cell wall components to recognition by and escape from murine macrophages. Infect Immun 78, 1650–1658 (2010). [PubMed: 20123707]
78. Ost KS, et al. Adaptive immunity induces mutualism between commensal eukaryotes. Nature (2021).
79. Staab JF & Sundstrom P Genetic organization and sequence analysis of the hypha-specific cell wall protein gene HWP1 of Candida albicans. Yeast 14, 681–686 (1998). [PubMed: 9639315]
80. Fonzi WA & Irwin MY Isogenic strain construction and gene mapping in Candida albicans. Genetics 134, 717–728 (1993). [PubMed: 8349105]
81. Prieto D, Román E, Correia I & Pla J The HOG pathway is critical for the colonization of the mouse gastrointestinal tract by Candida albicans. PLoS One 9, e87128 (2014). [PubMed: 24475243]
82. Park YN & Morschhäuser J Tetracycline-inducible gene expression and gene deletion in Candida albicans. Eukaryot Cell 4, 1328–1342 (2005). [PubMed: 16087738]
83. Noble SM & Johnson AD Strains and strategies for large-scale gene deletion studies of the diploid human fungal pathogen Candida albicans. Eukaryot Cell 4, 298–309 (2005). [PubMed: 15701792]
84. Granger BL, Flenniken ML, Davis DA, Mitchell AP & Cutler JE Yeast wall protein 1 of Candida albicans. Microbiology (Reading) 151, 1631–1644 (2005). [PubMed: 15870471]
85. Román E, Coman I, Prieto D, Alonso-Monge R & Pla J Implementation of a CRISPR-Based System for Gene Regulation in *Candida albicans*. mSphere 4, e00001–00019 (2019). [PubMed: 30760608]
86. Chauvel M, et al. A Versatile Overexpression Strategy in the Pathogenic Yeast Candida albicans: Identification of Regulators of Morphogenesis and Fitness. PLOS ONE 7, e45912 (2012). [PubMed: 23049891]
87. Pla J, Pérez-Díaz RM, Navarro-García F, Sánchez M & Nombela C Cloning of the Candida albicans HIS1 gene by direct complementation of a C. albicans histidine auxotroph using an improved double-ARS shuttle vector. Gene 165, 115–120 (1995). [PubMed: 7489899]
88. Xie J, et al. White-Opaque Switching in Natural MTLa/α Isolates of Candida albicans: Evolutionary Implications for Roles in Host Adaptation, Pathogenesis, and Sex. PLOS Biology 11, e1001525 (2013). [PubMed: 23555196]

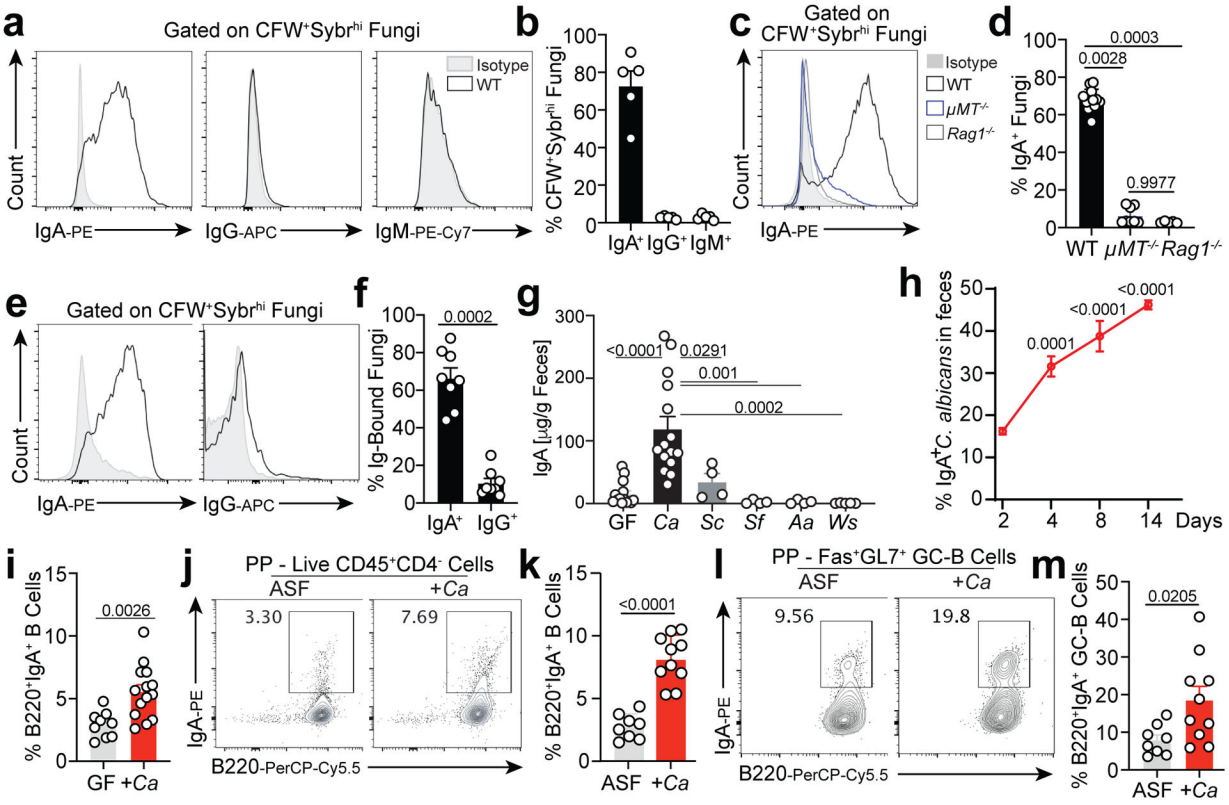

Figure 1. Under homeostatic conditions, the majority of the mouse and human gut mycobiota is coated by secretory IgA primarily induced by *C. albicans*.

a-b, Frequency of IgA-, IgG-, and IgM-bound fungi within the Sybr^{hi}CFW^{+} fraction of feces collected from SPF WT WCM-CE mice, assessed by flow cytometry. Gray curves in (a) represent corresponding Ig-isotype control staining. Data representative of three independent experiments. $N = 5$. **c-d,** Frequency of IgA-bound fungi assessed in WCM-CE SPF mouse feces from *Rag1*$^{-/-}$ and B cell-deficient *μMT*$^{-/-}$ mice in comparison with WT mice. Filled-in gray curve in (c) represent IgA-isotype control staining. Data represents two independent experiments. Kruskal-Wallis test followed by Dunn's multiple comparisons test. WT, $N = 13$; *μMT*$^{-/-}$, $N = 8$; *Rag1*$^{-/-}$, $N = 5$. **e-f,** Feces collected from healthy human individuals assessed for IgA- and IgG-bound fungi by flow cytometry. Gray curves in (e) represent IgA-isotype control staining. Two-sided Mann Whitney test. $N = 8$. **g,** Total free sIgA levels in the feces of germ-free (GF) mice monocolonized with common commensal and dietary fungal species. Data representative of two independent experiments. Kruskal-Wallis test followed by Dunn's multiple comparisons test. GF, $N = 12$; *C. albicans*, $N = 15$; *S. cerevisiae*, $N = 4$; *S. fibuligera*, $N = 4$; *A. amstelodami*, $N = 4$; *W. sebi*, $N = 5$. **h**, Germ-free (GF) mice were orally gavaged with *C. albicans* (*+Ca*) and sIgA binding to intestinal *C. albicans* was observed by flow cytometry in feces collected at days 2-, 4-, 8-, and 14-days post-colonization. Analysis of IgA binding representative of two independent experiments; one-way ANOVA, followed by Sidak's test, N=6. **i,** Germ-free (GF) mice were orally gavaged with PBS (GF) or colonized for two weeks with *C. albicans* (*+Ca*). PP of all mice were harvested at day 14 for flow cytometry analysis of frequency of B220^{+}IgA^{+} among Live CD45^{+}CD4^{-} cells (i). Pooled from two independent experiments; two-sided

Mann Whitney test (i). GF, $N = 9$; +*Ca*, $N = 14$. **j-m,** Representative plots and flow cytometry analysis of frequency of $B220^{+}IgA^{+}$ in PP B cells (j-k) and germinal center B cell (GC-B, l-m) subset in the PP of mycobiota-free altered Schaedler flora (ASF) mice orally gavaged with PBS (ASF) or colonized for two weeks with *C. albicans* (+*Ca*). Pooled from two independent experiments; two-sided Mann Whitney test. ASF, $N = 8$; +*Ca*, $N = 10$. Dots, fecal samples/gut-associated lymphoid cells (GALT) of individual mice (**a-d, g, i, j, k l, m**) or healthy humans (**e-f**); error bars, SEM. ns-$p \geq 0.05$, *$p < 0.05$, **$p < 0.01$, ***$p < 0.001$, ****$p < 0.0001$.

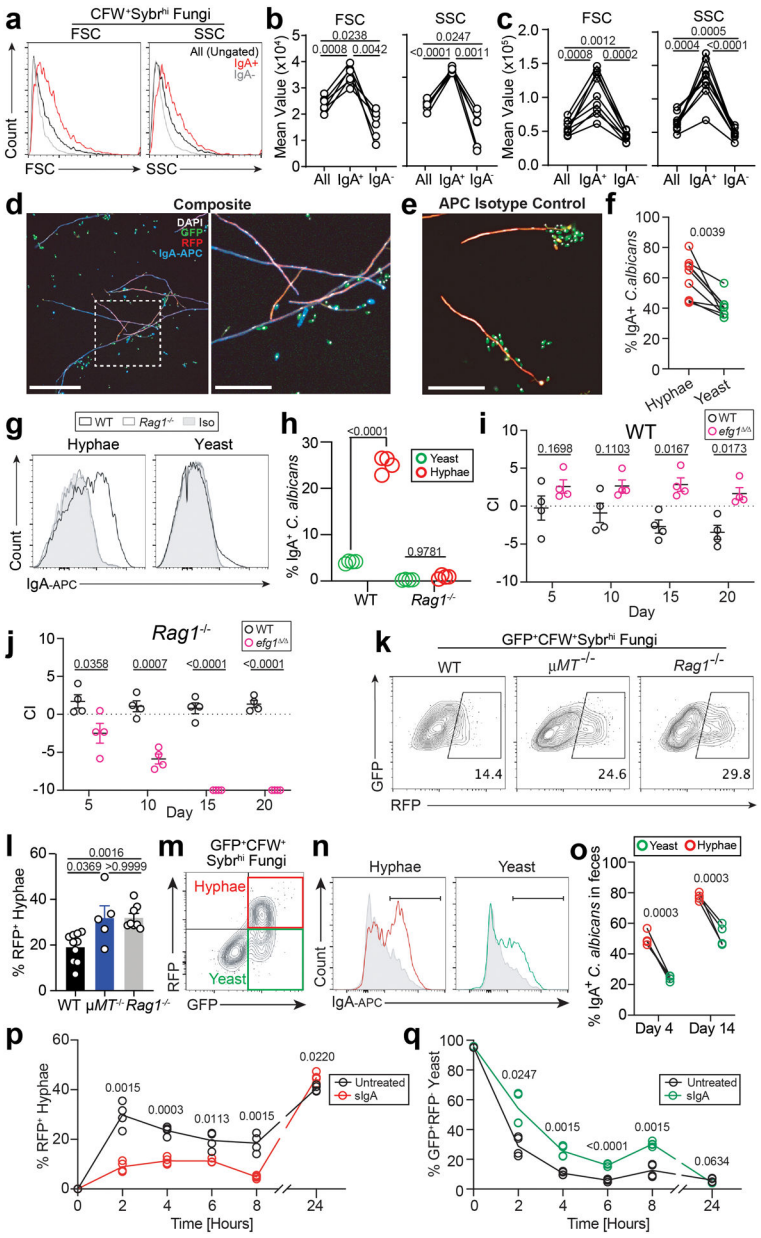

Figure 2. Secretory IgA antibodies preferentially bind fungal hyphae and influence *C. albicans* morphotypes in the gut.

a-b, Representative plots of forward scatter (a, left) and side scatter (a, right), analysis (b) of all CFW^{+}Sybr^{hi} fungi (All), and the IgA^{+} / IgA^{-} fungal fractions, collected from healthy human fecal samples. Mixed effects analysis with Geisser-Greenhouse correction. $N = 6$. **c,** SPF-WT JAX mice were fed with 1×10^{8} *C. albicans* and feces were collected four days later. Average forward scatter (left) and side scatter (right) values of all CFW^{+}Sybr^{hi} fungi (All), as well as the IgA^{+} and IgA^{-} CFW^{+}Sybr^{hi} fractions. Mixed effects analysis with Geisser-Greenhouse correction. $N = 8$. **d-f,** Immunofluorescence microscopy of Ca-dREP incubated with human fecal supernatant as a source of sIgA, stained with DAPI and anti-human IgA-APC (d) or an APC isotype control (e). GFP^{+}RFP^{-} yeast, GFP^{+}RFP^{+} hyphae, and IgA^{+} events for each were counted calculation of IgA-coating frequency by

morphotype (f). Composite images of 20X magnification and zoomed-in dotted regions of each are shown in left and right panels, respectively. Single channels are shown in Extended Data Fig. 3 (top rows). Scale bar represents 50μm in 20X panel and 20μm in zoomed-in panel. Data representative of three independent experiments. Two-tailed Wilcoxon matched pairs signed rank test. **g-h,** Ca-dREP were cultured for 18 hours in hyphae-inductive media and stained with fecal supernatant from *C. albicans*-colonized IgA-sufficient WT or IgA-deficient *Rag1*$^{-/-}$ mice, followed by sIgA staining. Representative plots (g) and analysis (h) of IgA binding from two independent experiments. Gray curves in (g) represent Ig-isotype control staining. Multiple two-tailed t tests. WT, $N = 4$. *Rag1*$^{-/-}$, $N = 4$. **i-j,** SPF-WT (i) and *Rag1*$^{-/-}$ (j) mice were treated with cefoperazone and colonized with a 1:1 mix of 1×10^8 *C. albicans* strain CAF2-RFP (WT, black) and *efg1*$^{\Delta/\Delta}$ (pink) *C. albicans*, after which CFUs of each were tracked for 20 days. For each mouse genotype, competition indices (CI) were generated for each strain, calculated as: CI = $\log_2$(recovered CFUs/original inoculum CFU). Multiple two-tailed t tests. WT, $N = 4$; *Rag1*$^{-/-}$, $N = 4$. Data representative of two independent experiments. **k-l,** Representative flow cytometry plots (k) and analysis (l) of RFP$^+$ hyphae in WT, *μMT*$^{-/-}$, and *Rag1*$^{-/-}$ feces of mice 4 days after cefoperazone-aided colonization with 1×10^8 Ca-dREP. Plots gated on Ca-dREP. Data representative of three independent experiments. Kruskal-Wallis test followed by Dunn's multiple comparisons test. WT, $N = 10$; *μMT*$^{-/-}$, $N = 5$; *Rag1*$^{-/-}$, $N = 8$. **m-o,** Quantification of IgA-coating and Ca-dREP morphotypes in SPF WT JAX mice feces 4 and 14 days after cefoperazone-aided colonization. Plots in (m) represent colon contents gated on CFW$^+$ events, with GFP$^+$RFP$^-$ yeast and GFP$^+$RFP$^+$ hyphae Ca-dREP populations easily distinguished. Connected dots in (o) represent % IgA$^+$ fungal cells within the hyphal (red) and yeast (green) Ca-dREP gates in a single fecal sample collected at day 4 or 14 respectively. Two-tailed Wilcoxon matched pairs signed rank test. $N = 7$. **p-q,** sIgA from healthy human feces was applied (5μg/well) at 0 and 6 hours to a two-partner system comprising of Ca-dREP and Caco-2 cells upon Ca-dREP infection. The frequency of hyphal (p) and yeast (q) morphologies was measured by flow cytometry using the gating strategy described in (m). Each dot represents a well. Multiple unpaired two-tailed t tests followed by Sidak's test. Error bars, SEM.

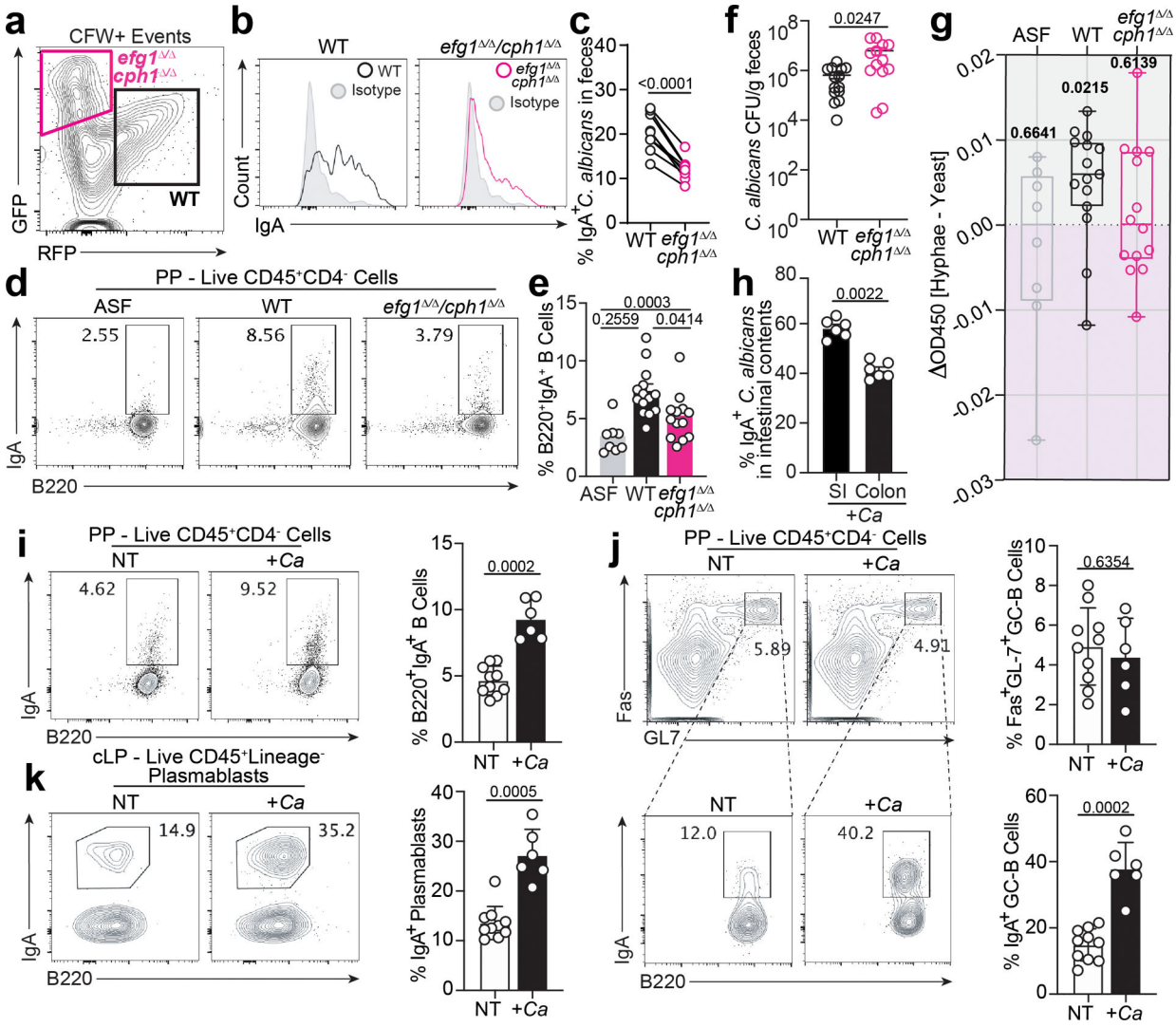

Figure 3. *C. albicans* hyphal morphotypes induce potent sIgA responses.

a-c, Feces collected from cefoperazone treated SPF-WT JAX mice 4 days after oral gavage with a 1:1 mixture of 1×10^8 CAF2-RFP and GFP$^+$ *efg1*$^{\Delta/\Delta}$/*cph1*$^{\Delta/\Delta}$ *C. albicans*. Representative flow cytometry plots of WT (black gate) and *efg1*$^{\Delta/\Delta}$/*cph1*$^{\Delta/\Delta}$ (pink gate) (a) and the IgA$^+$ gates within each (b), quantified as the IgA-bound fraction for each strain. Gray curves in (b) represent Ig-isotype control staining (iso). *C. albicans* in feces plotted in (a) is gated on CFW$^+$Sybr^{hi} population. Data from two independent experiments. Dots represent analyses of IgA binding in each *C. albicans* strain found in the same sample. Two-tailed Wilcoxon matched pairs signed rank test. $N = 8$. **d-g,** Flow cytometry representative plots (d), analysis (e) of frequency of B220$^+$IgA$^+$ among Live CD45$^+$CD4$^-$ cells in the PP of ASF-WT mice and *C. albicans* burdens (f) two weeks after oral colonization with either WT *C. albicans* (+*Ca*) or *efg1*$^{\Delta/\Delta}$*cph1*$^{\Delta/\Delta}$ yeast-locked *C. albicans* (*efg1*$^{\Delta/\Delta}$*cph1*$^{\Delta/\Delta}$). Free fecal sIgA reactivity was compared between WT *C. albicans* hyphae and yeast lysates by ELISA (g). Values graphed = OD450[hyphae] – OD450[yeast]. Pooled from two independent experiments; Kruskal-Wallis test followed by Dunn's multiple comparisons test (e) and two-tailed Wilcoxon Signed Rank Test (f). ASF, $N = 8$; WT, $N = 14$; Δ*efg1*/Δ*cph1*,

N = 13. **h-k,** sIgA binding to intestinal *C. albicans* in colon and small intestinal (SI) contents was measured (h), and Peyer's patches (PP) B cells and colonic lamina propria (cLP) plasmablasts were assessed for IgA^+ class-switch recombination (CSR) in SPF-WT JAX mice after two weeks of cefoperazone-aided colonization with WT *C. albicans* (+*Ca*) relative to untreated controls (NT). Representative plots and analysis of PP $B220^+IgA^+$ B cells (i), Fas^+GL7^+ germinal center B cells (GC-B) and IgA^+ GC-B cells (j). $B220^-IgA^+$ plasmablasts in the colonic lamina propria (cLP) are shown (k). Two samples were excluded from the +*Ca* experimental group due to failed fluorescent staining. Two-tailed Mann-Whitney test. NT, *N* = 10; +*Ca*, *N* = 8. Box in (g) shows 25^{th} and 75^{th} percentiles with middle horizontal line and whiskers representing the median and min/max, respectively. Error bars, SEM.

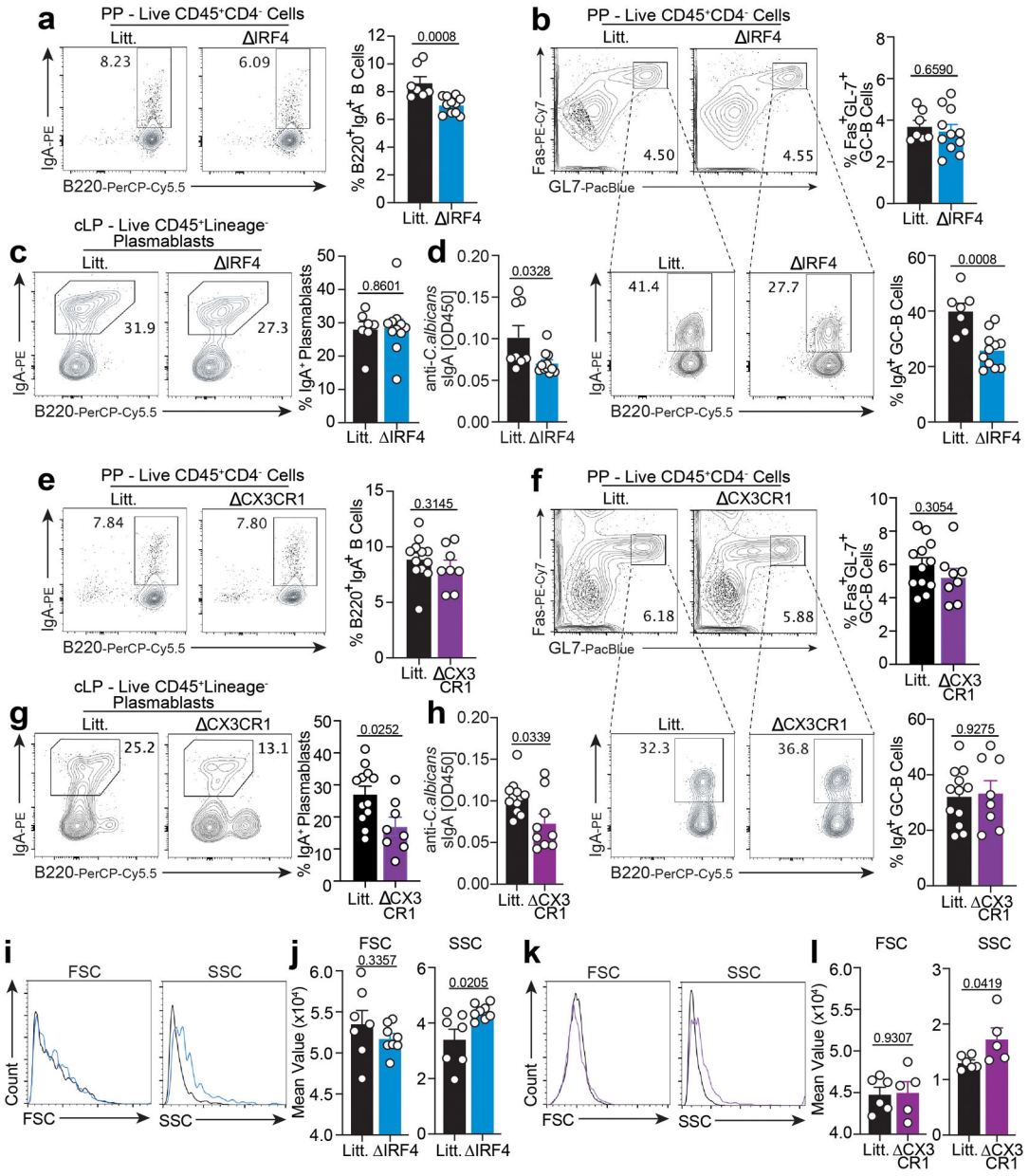

Figure 4. *C. albicans* sIgA responses are mediated through interaction with DC2 and CX3CR1^{+} MNPs.

Peyer's patches (PP) B cells and colonic lamina propria (cLP) plasmablasts were assessed for IgA^{+} class-switch recombination (CSR) after two weeks of cefoperazone-aided colonization with WT *C. albicans* in *Cd11c-cre*$^{+/-}$ × *IRF4*$^{fl/fl}$ (ΔIRF4; a-c) or *Cd11c-cre*$^{+/-}$ × *Cx3cr1*^{DTR} (ΔCX3CR1; e-g) SPF mice relative to *Cd11c-cre*$^{-/-}$ littermates (Litt.). Representative plots and analysis of PP B220^{+}IgA^{+} B cells (a, e), Fas^{+}GL7^{+} germinal center B cells (GC-B), and IgA^{+} GC-B cells (b, f). Representative plots and analyses of B220^{-}IgA^{+} plasmablasts in the lamina propria (cLP) are shown in (c, g). d, h. ELISA-based characterization of luminal anti-*C. albicans* sIgA in small intestines of ΔIRF4 (d), ΔCX3CR1(h) mice and the respective littermates after two weeks of intestinal colonization by WT *C. albicans*. Representative plot of side and forward scatter (i, k) and respective

analysis (j, l) of $CFW^{+}Sybr^{hi}$ *C. albicans* (gated as shown in Extended Figure 4c) in luminal content of ΔIRF4 (i, j), ΔCX3CR1(k, l) mice and the respective littermates. Mixed effects analysis with Geisser-Greenhouse correction. Data represents 2 or 3 independent experiments. Two-tailed Mann-Whitney test. ΔIRF4, $N = 12$*; Litt., $N = 7$; ΔCX3CR1, $N = 8$; Litt., $N = 12$. *One sample was excluded from the ΔIRF4 experimental group due to failed fluorescent staining. Error bars, SEM.

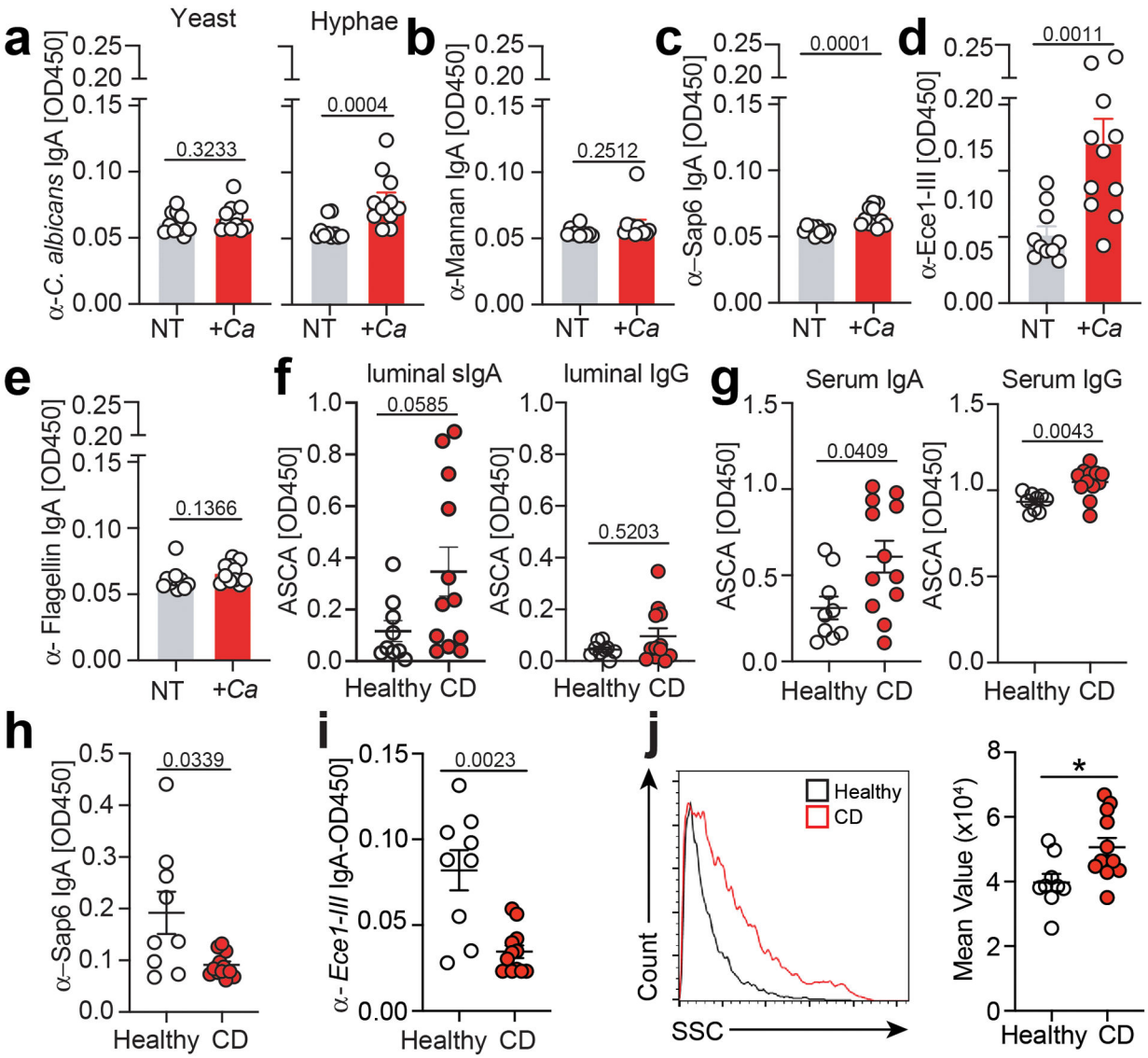

Figure 5. *C. albicans*-induced sIgA that target hyphae-associated virulence factors are decreased in CD patients.

a-e, Characterization of sIgA in feces of ASF-WT mice with (+*Ca*) or without (NT) two weeks of intestinal colonization by WT *C. albicans*. Reactivity assessed by ELISA against lysates from WT *C. albicans* hyphae and yeast (a), fungal cell wall mannan (b), hyphae-associated virulence factors Sap6 (c) and candidalysin (*Ece1-III*) (d), and bacterial flagellin (e). Data represents 3 experiments, two-tailed Mann-Whitney test. NT, $N = 10$; *+Ca*, $N = 11$. **f-g**, Characterization of ASCA sIgA and IgG in mucosal washings (f) and serum (g) of healthy individuals and CD patients. Two-tailed Mann-Whitney test. Healthy, $N = 9$; CD, $N = 12$. **h-i,** Characterization of sIgA reactivity from mucosal washings of healthy individuals and CD patients against Sap6 (h), and candidalysin (i). Two-tailed Mann-Whitney test. Healthy, $N = 9$; CD, $N = 12$. **j,** Representative plot of side scatter (j, left) and respective analysis (j, right) exploring granularity of CFW^{+} $Sybr^{hi}$ fungi in mucosal washings of healthy individuals and CD patients. Healthy, $N = 9$; CD, $N = 12$. Each dot represents an

individual human subject, analysis performed with Two-tailed Mann-Whitney test followed by Benjamini-Hochberg (BH) correction. Error bars, SEM.